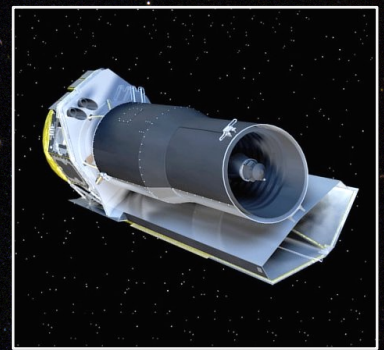
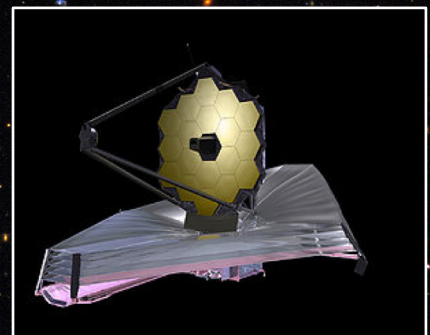
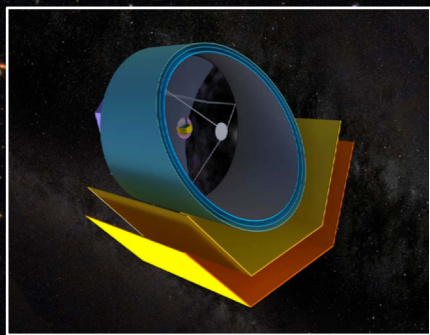


# Dust, PAHs, and Star Formation with future outlook for current and upcoming NASA missions

Irene Shvai

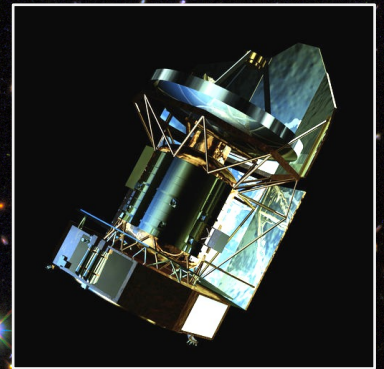
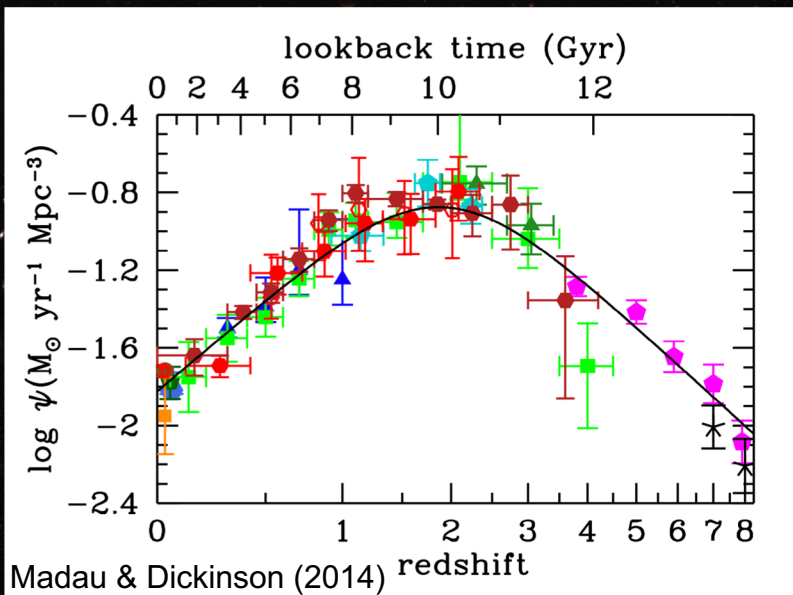
Hubble fellow, University of Arizona



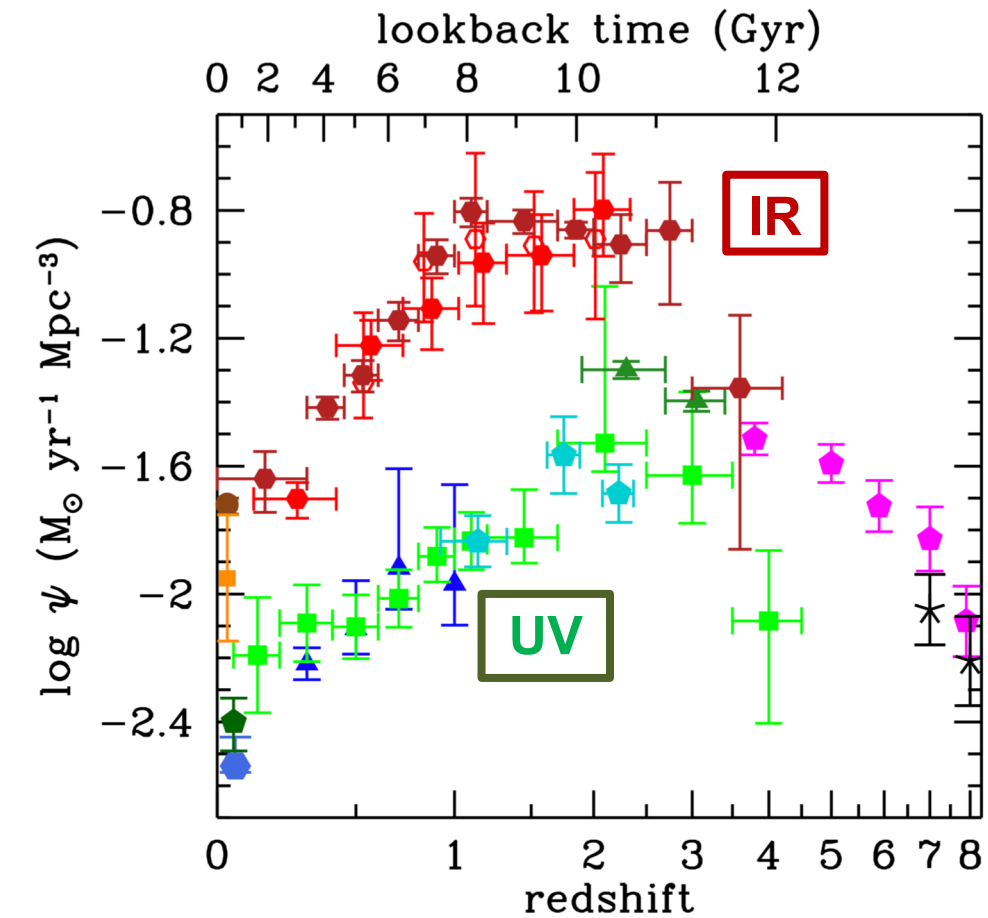
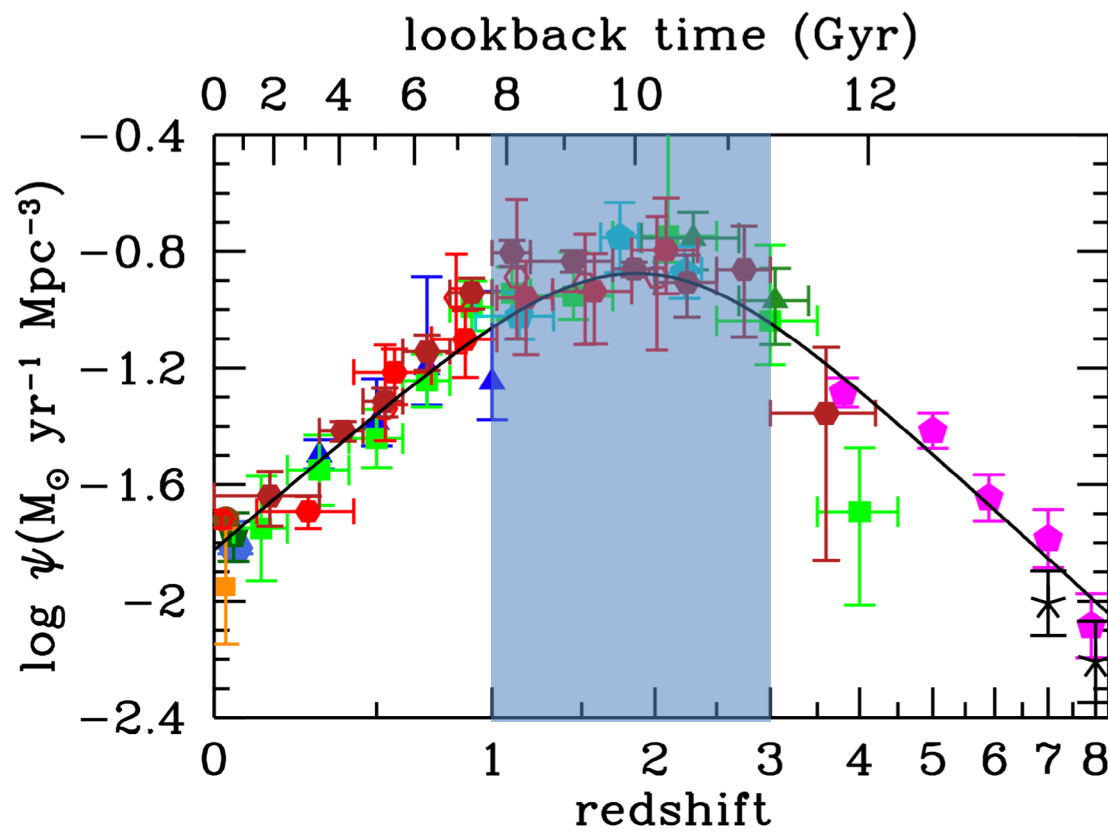


## Determining the evolution of the infrared universe

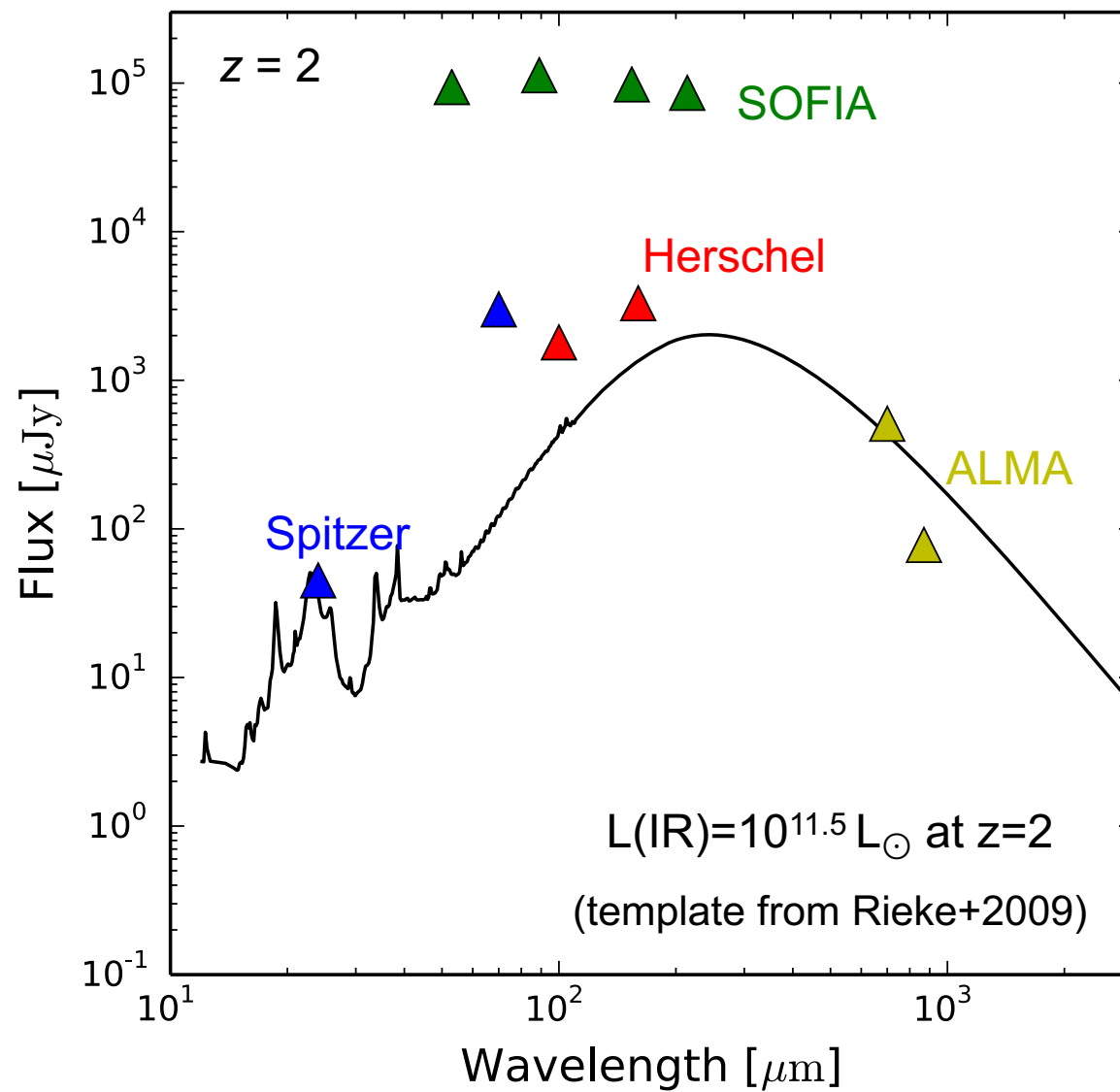
- Obscured Star Formation
- Dust and ISM
- AGN



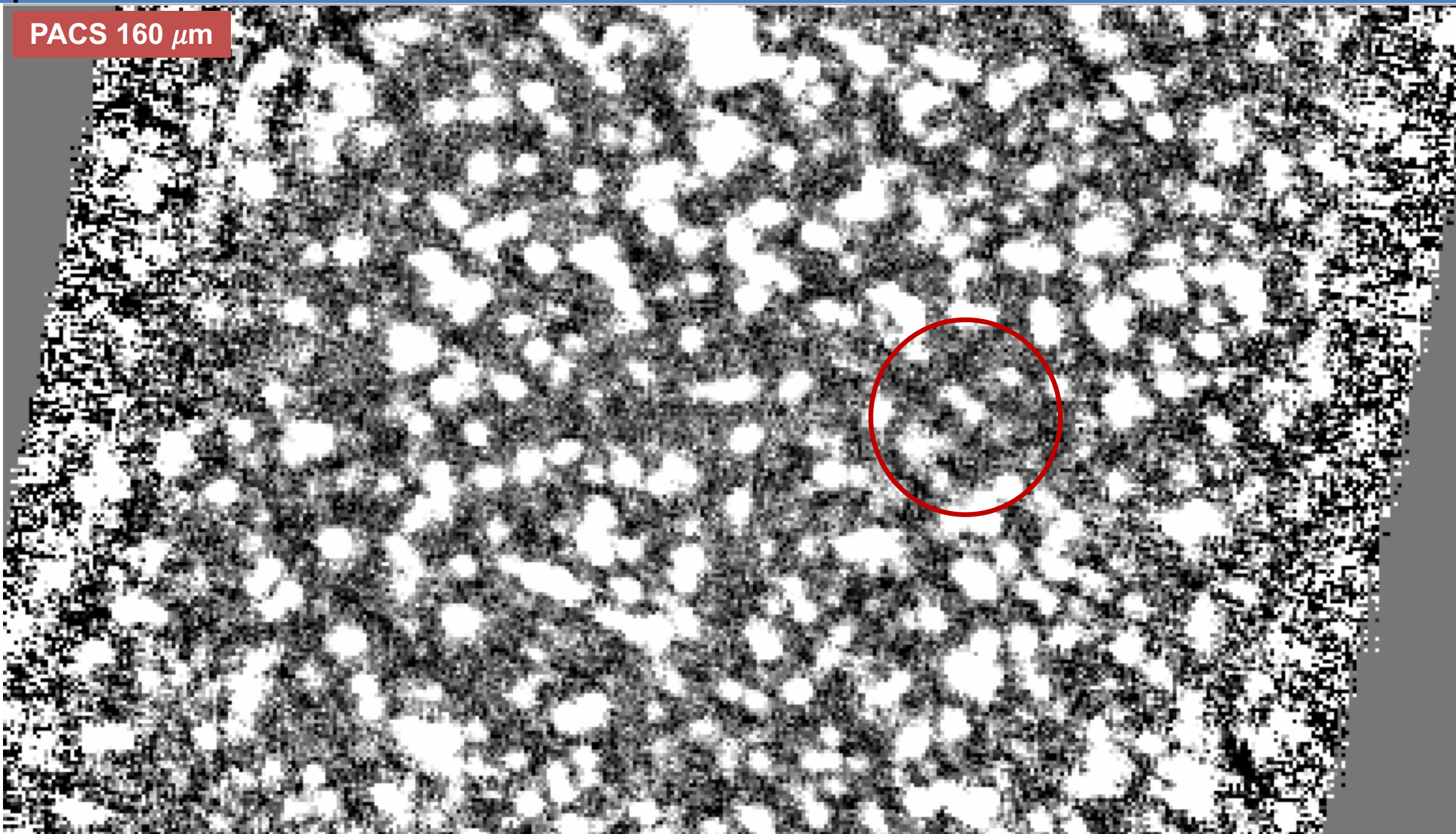
A significant fraction of our universe at all epochs is dominated by infrared emission

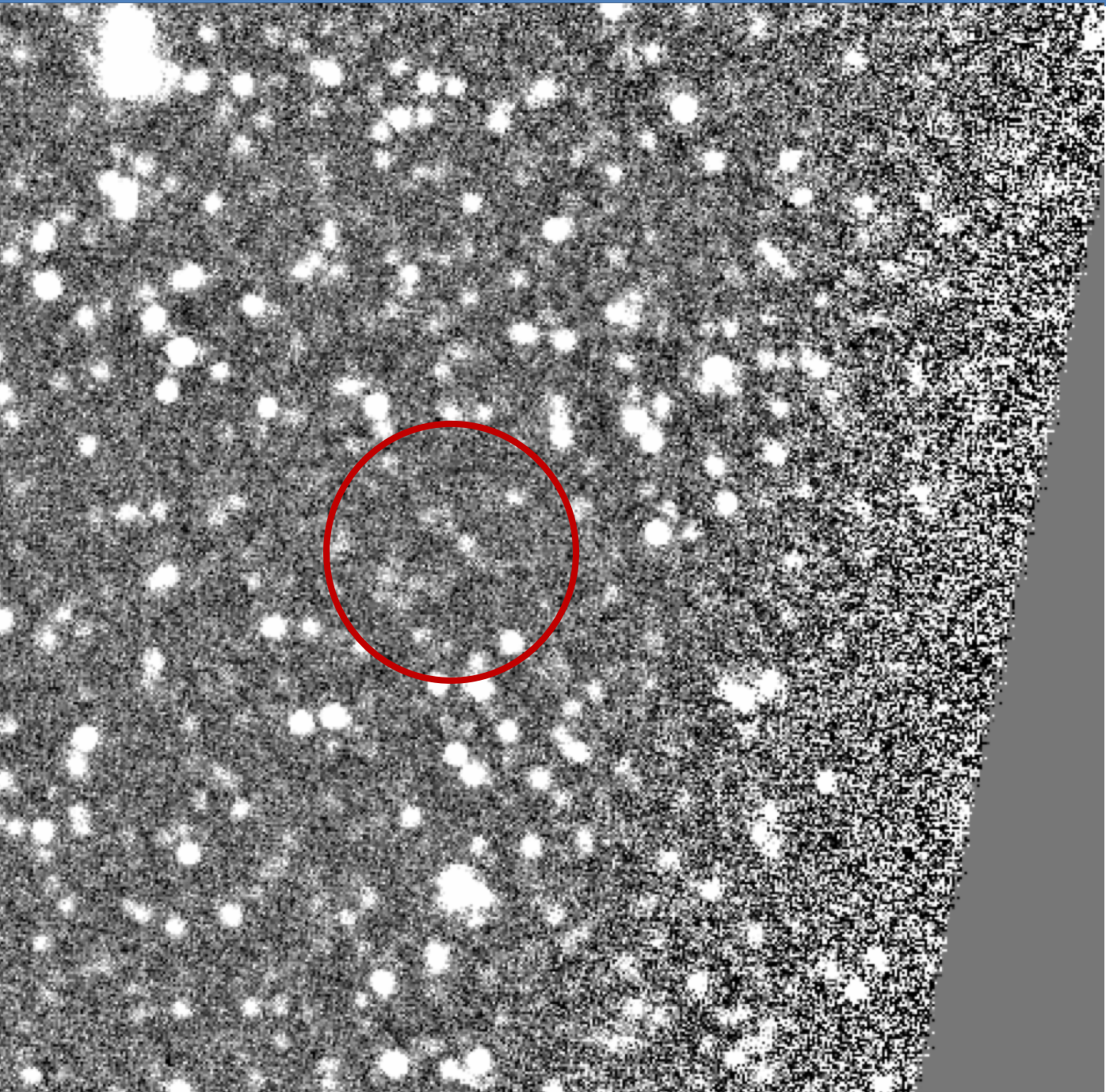
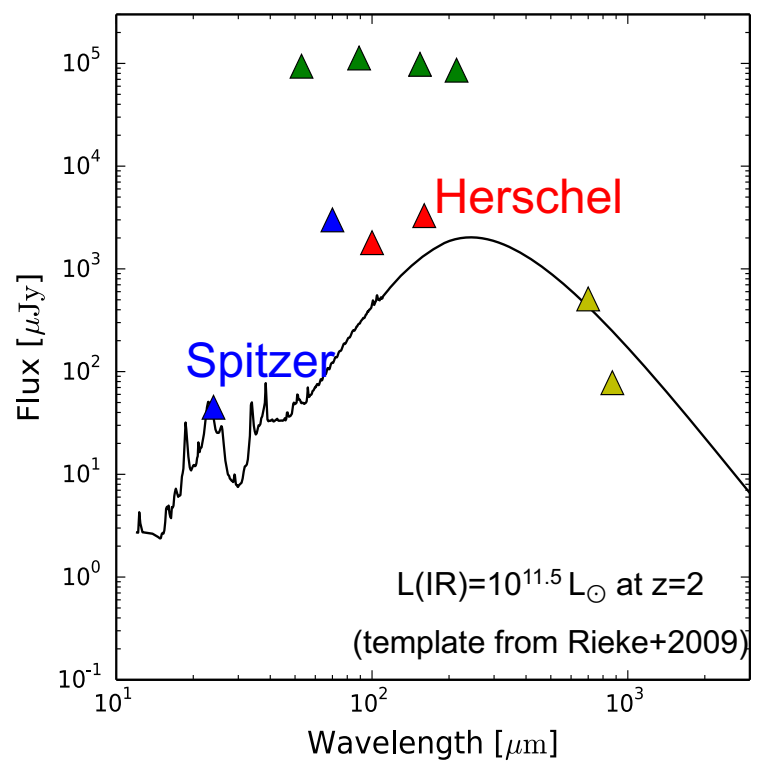


## How can we capture infrared light at intermediate redshifts?

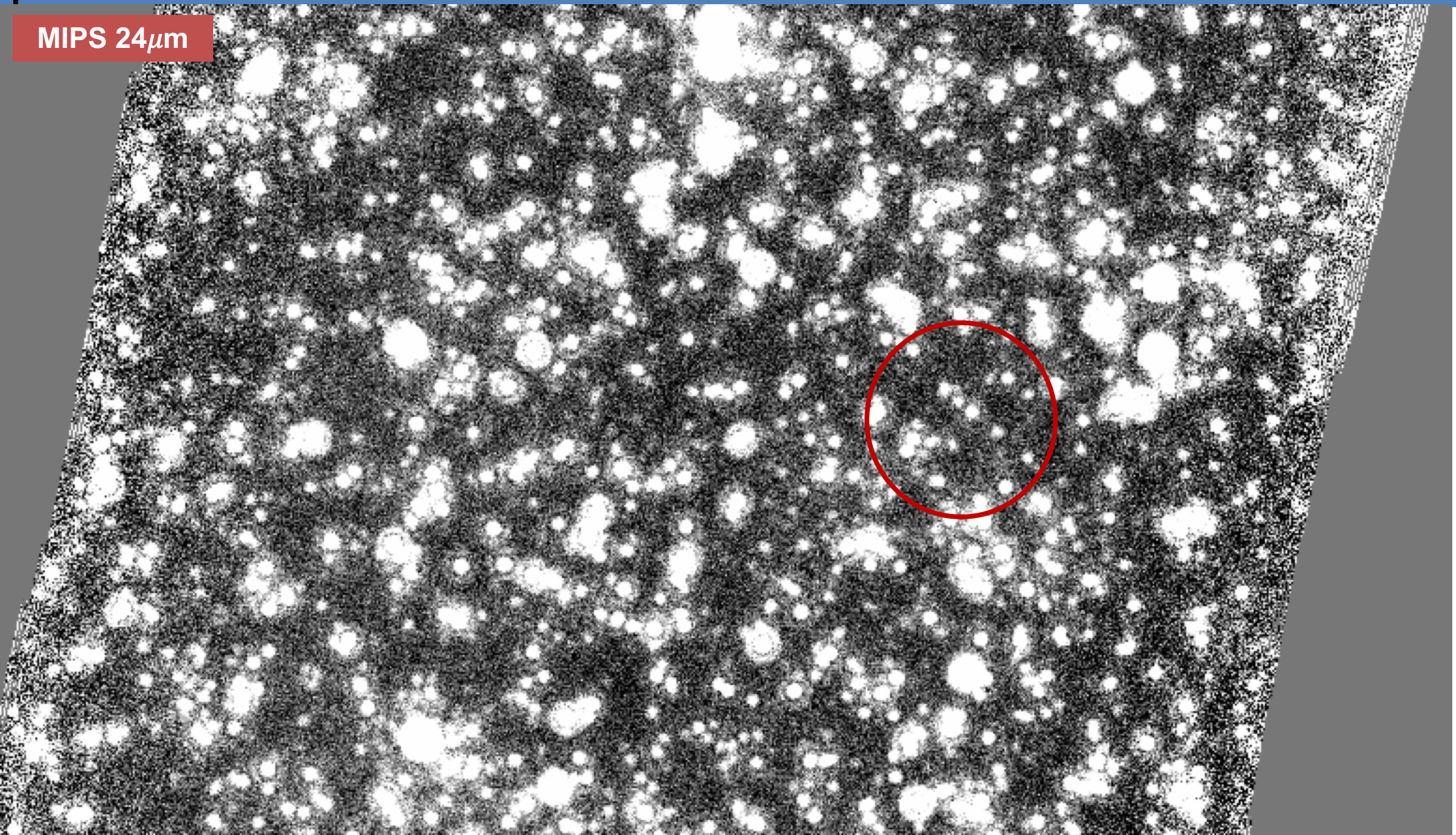


PACS 160  $\mu\text{m}$

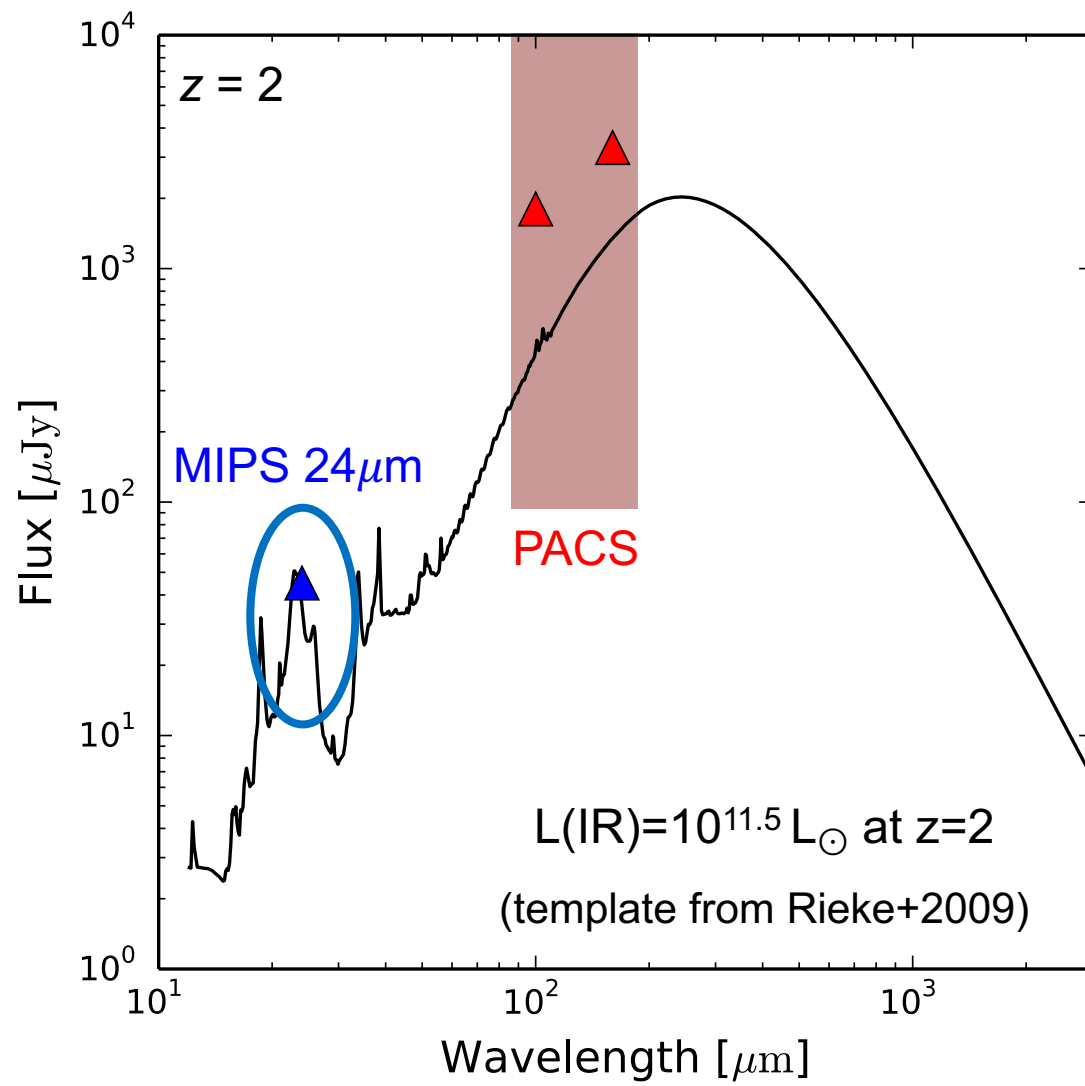
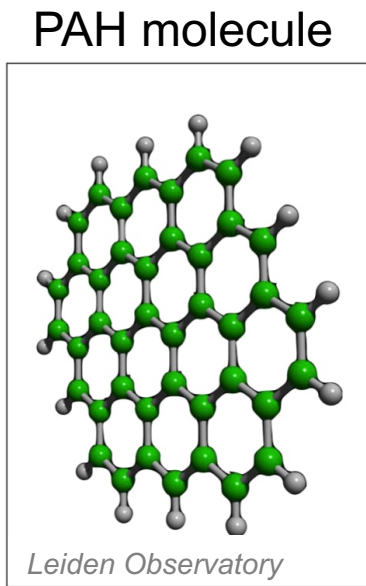


**PACS 100  $\mu\text{m}$** 

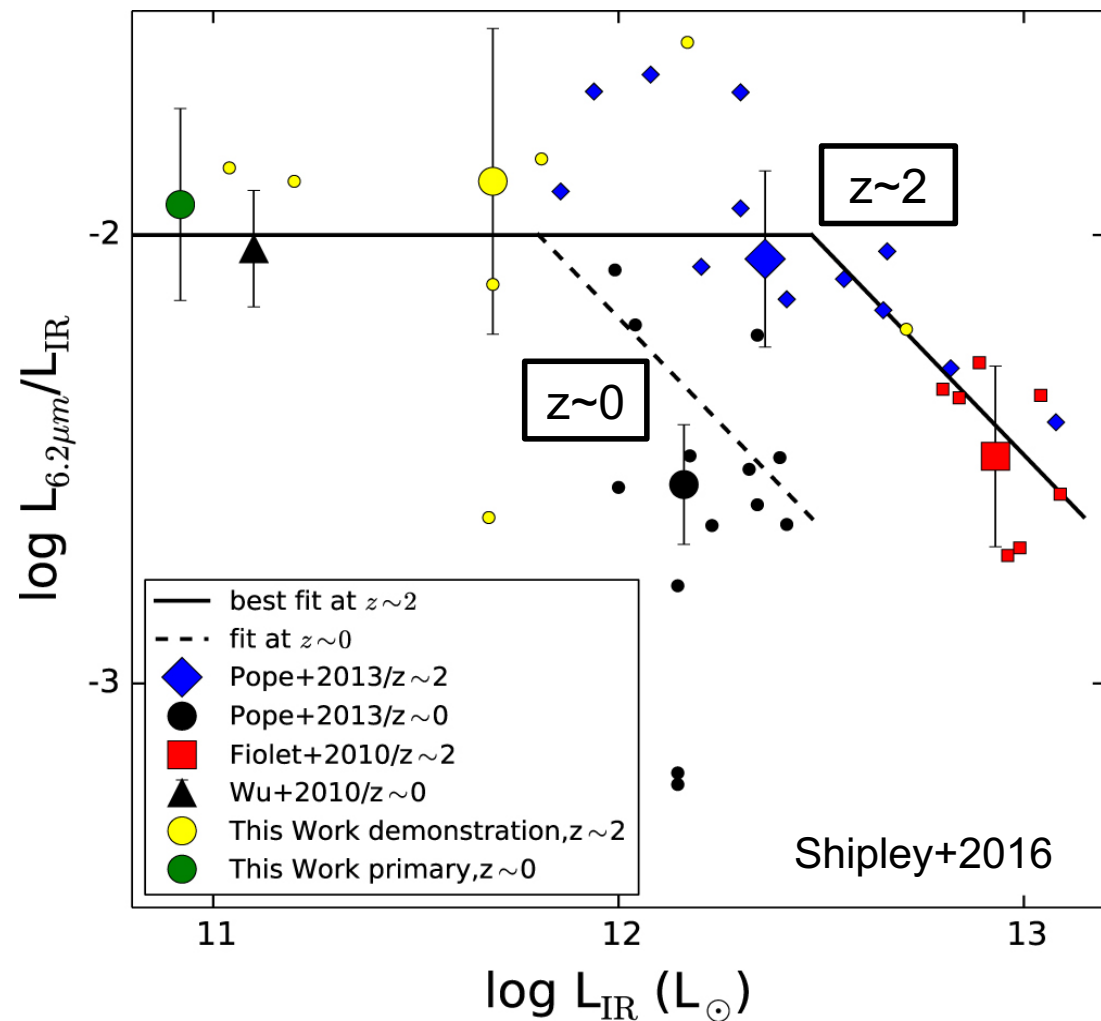
MIPS 24 $\mu$ m



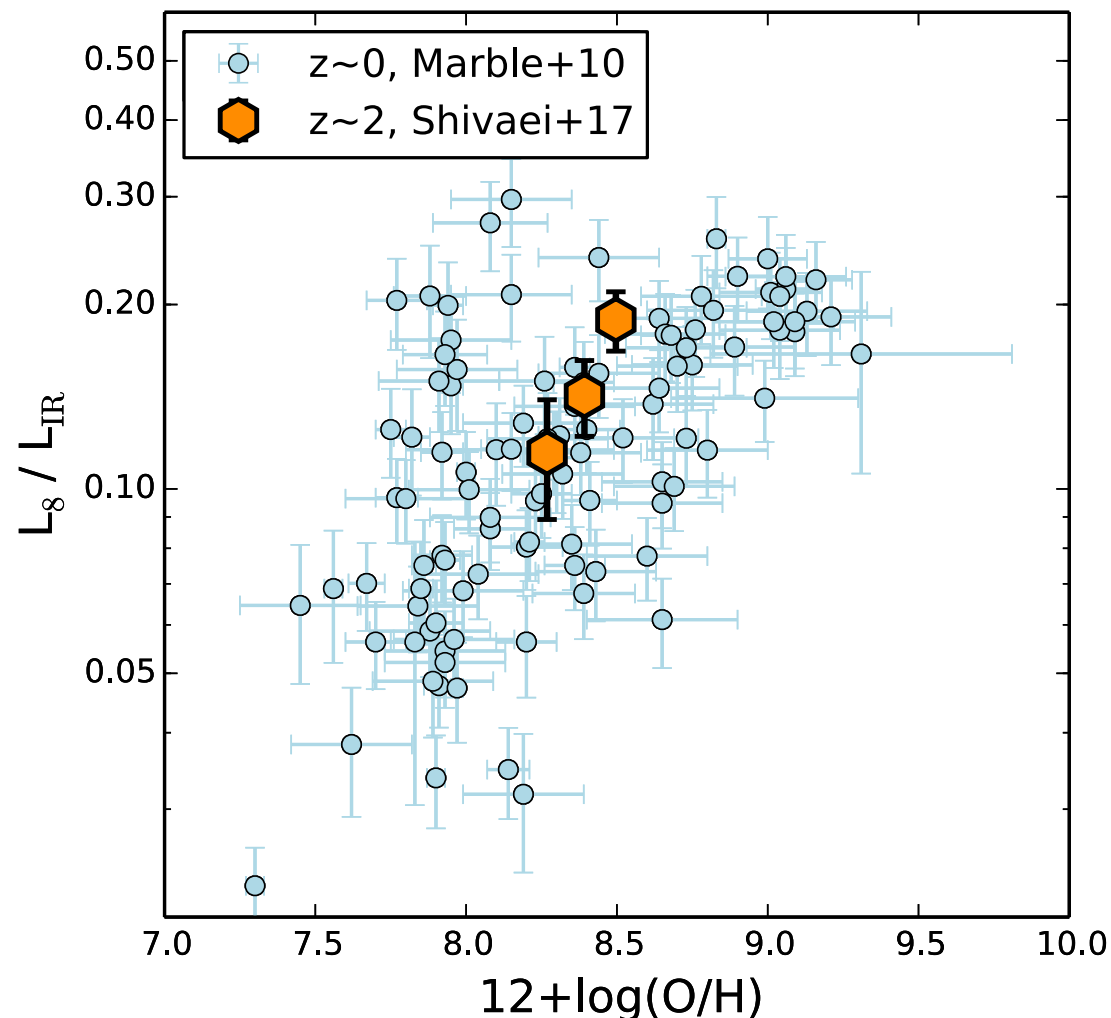
PACS bands trace the thermal IR emission, while MIPS 24 $\mu\text{m}$  traces the PAH emission



# The PAH luminosity suppression at high luminosities is redshift dependent

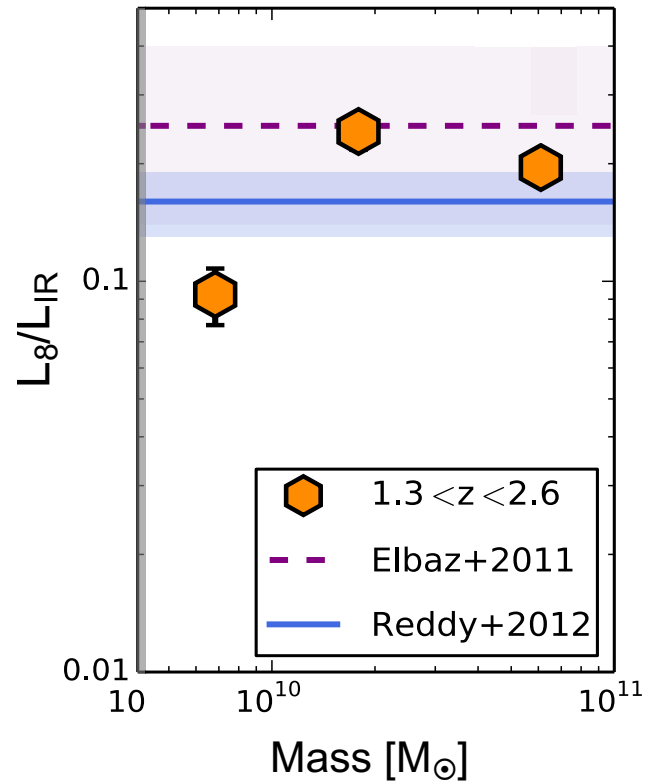
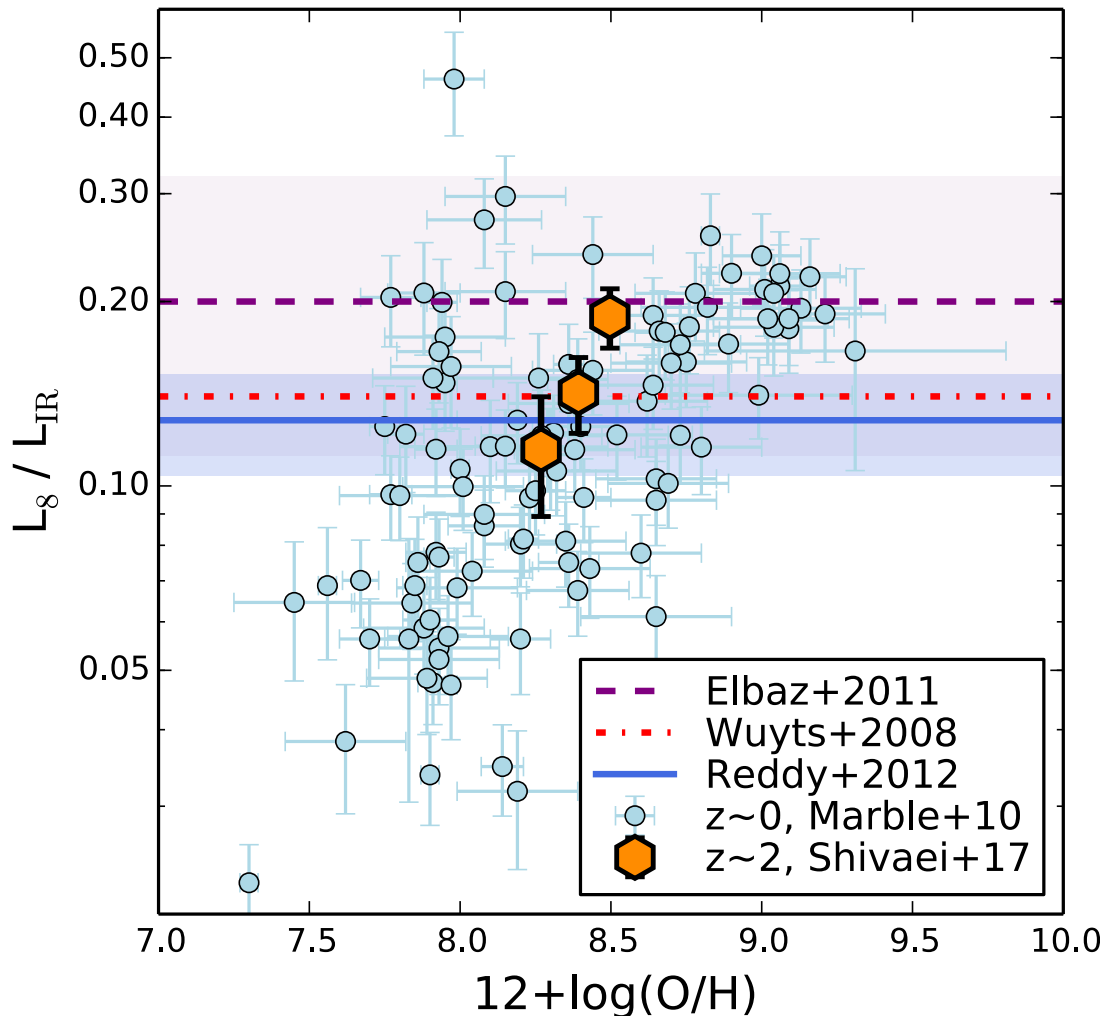


## PAH intensity scales with metallicity



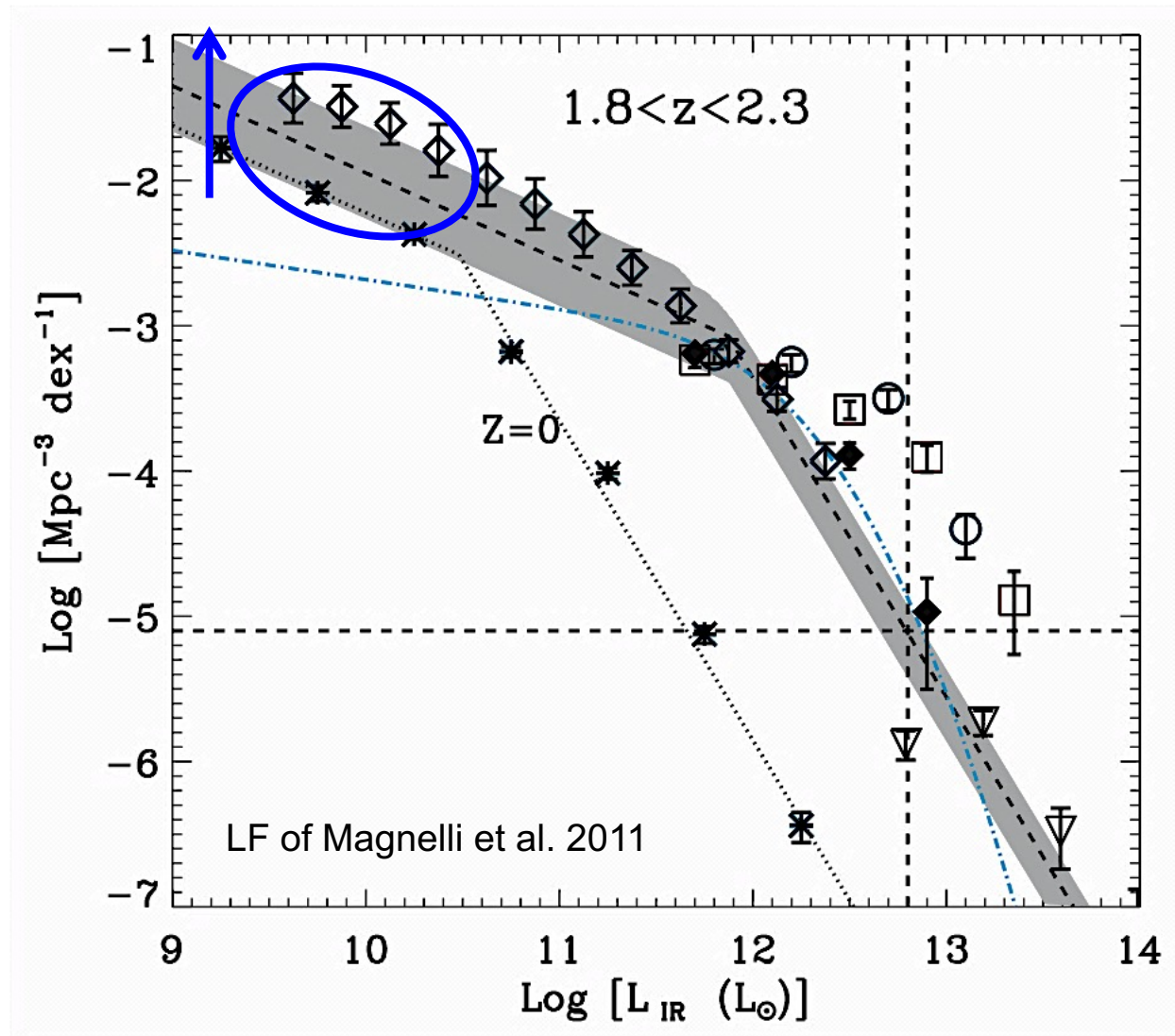
- Paucity of PAH molecules in low-metallicity environments
- Preferential destruction of PAH molecules in environments with hard and intense radiation

At low mass and low metallicities, single conversions of 7.7um to L(IR) underestimate the L(IR) and SFR(IR) by a factor of  $\sim 2$



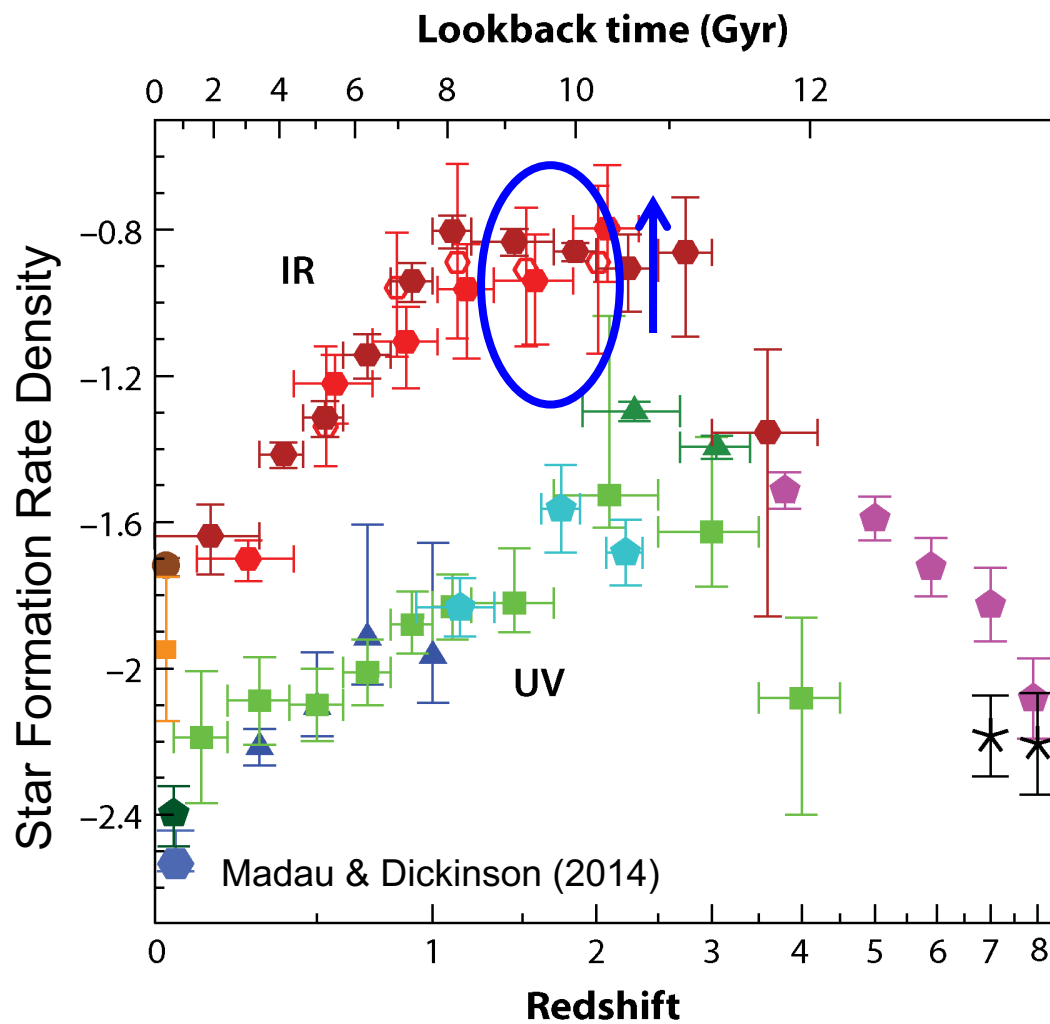
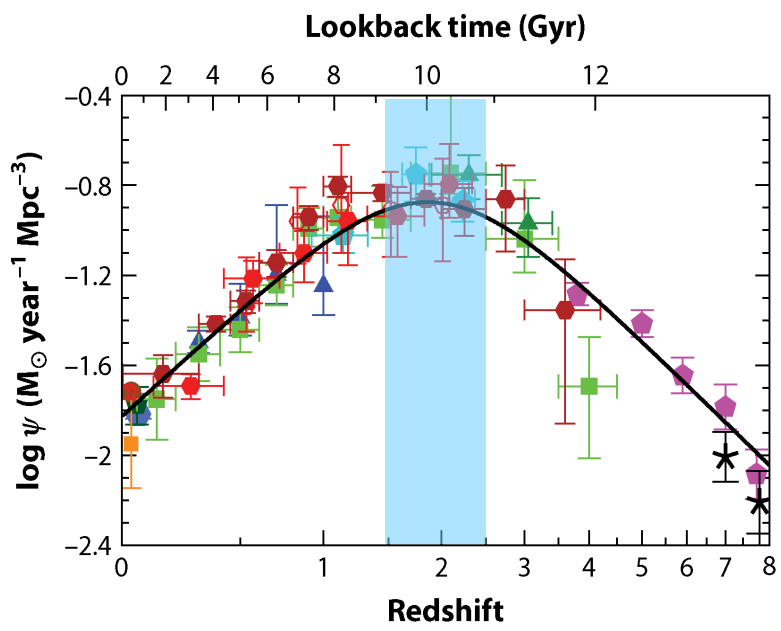
## The IR luminosity density at $z \sim 2$

30% increase in the IR luminosity density at  $z \sim 2$



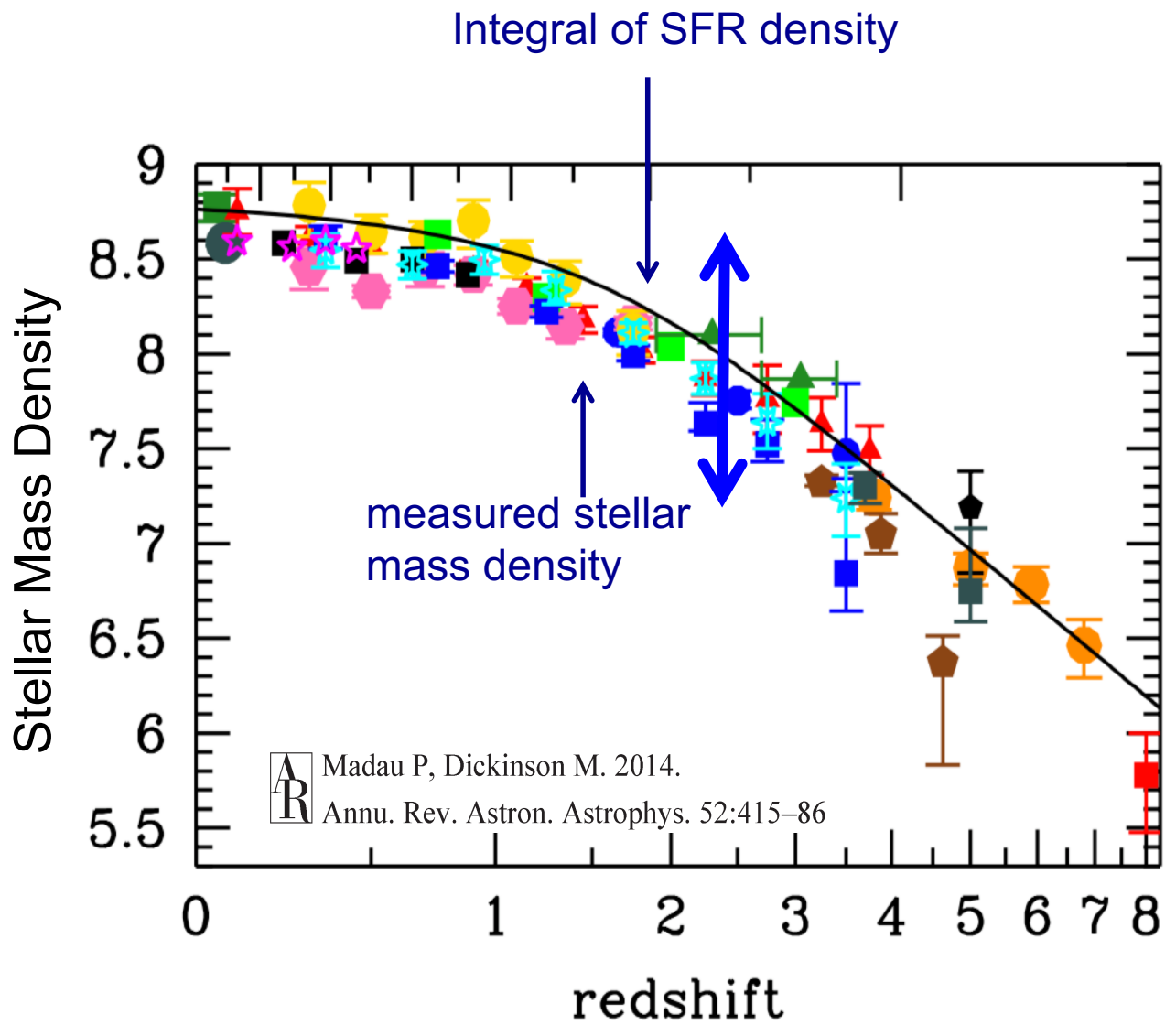
## The SFR Density at $z \sim 2$

30% increase in the SFR density  
at  $z \sim 2$

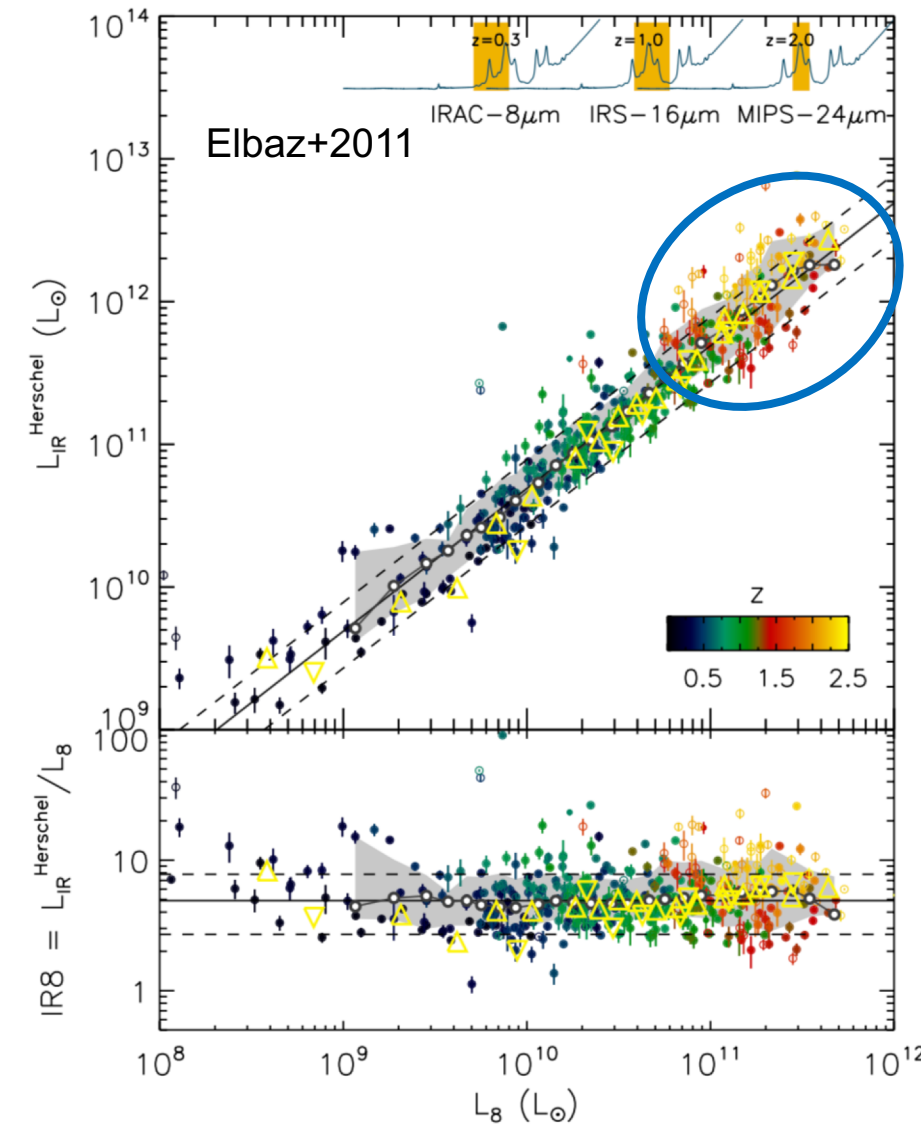
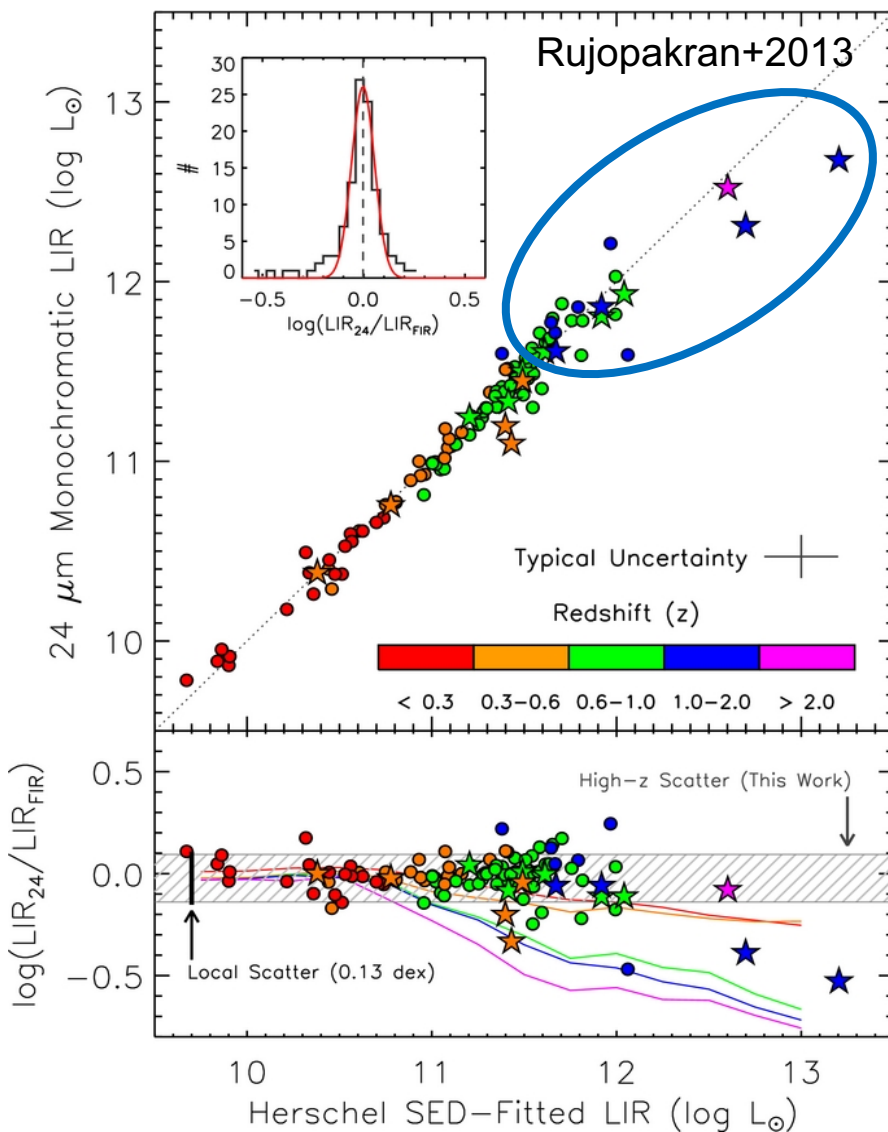


## Stellar Mass Density at $z \sim 2$

- Reinstates the discrepancy between the measured stellar mass density and the integral of SFR density over time



# PAH conversion to IR luminosity

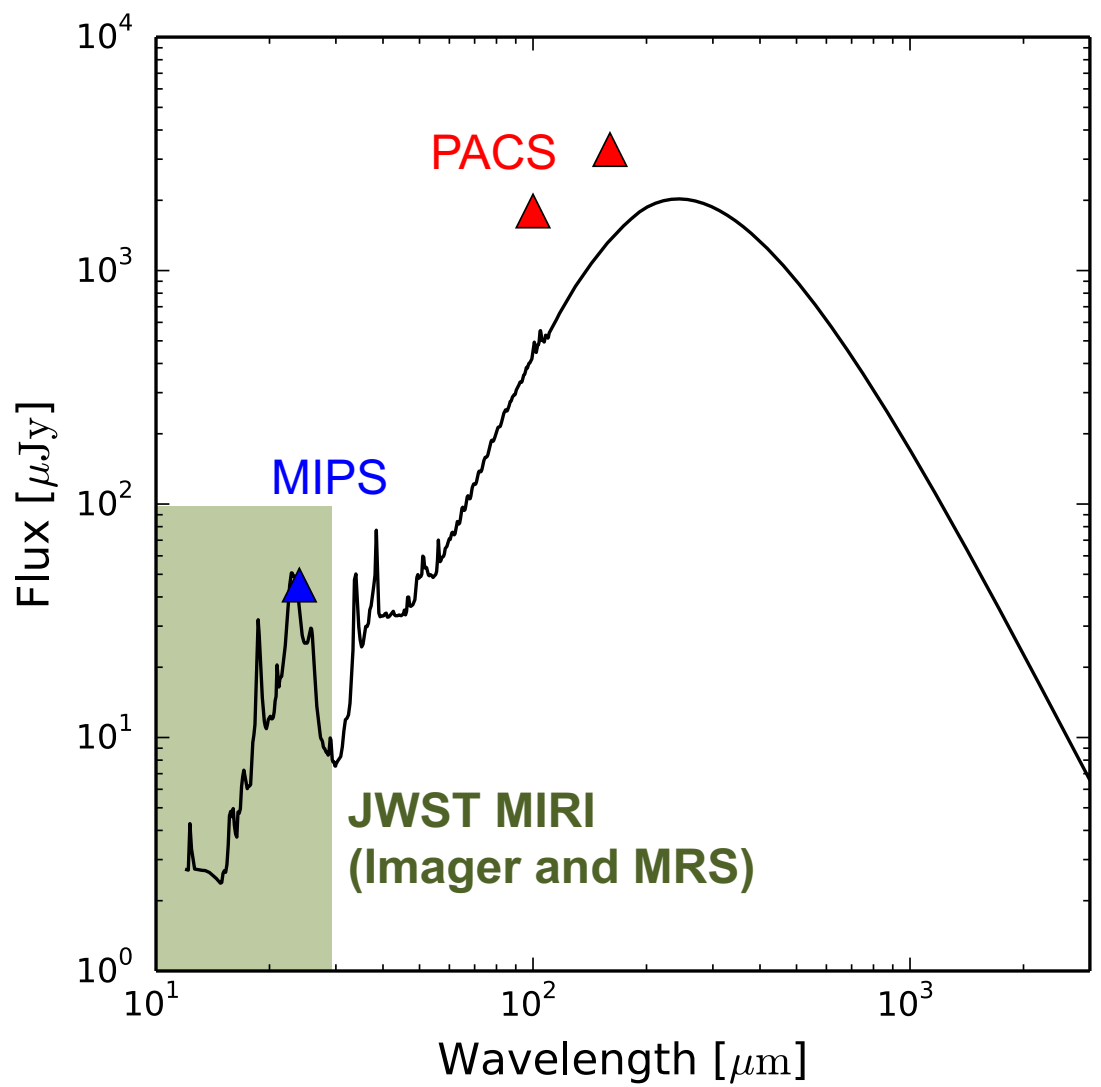


See also: Kennicutt & Evans (2012), Reddy et al. (2012), Wuyts et al. (2008), Bavouzet et al. (2008), Rigby et al. (2008), Caputi et al. (2007)

# JWST Mid-Infrared Instrument (MIRI)

Imaging and spectroscopy at  $\lambda = 4.9 - 28.8 \mu\text{m}$

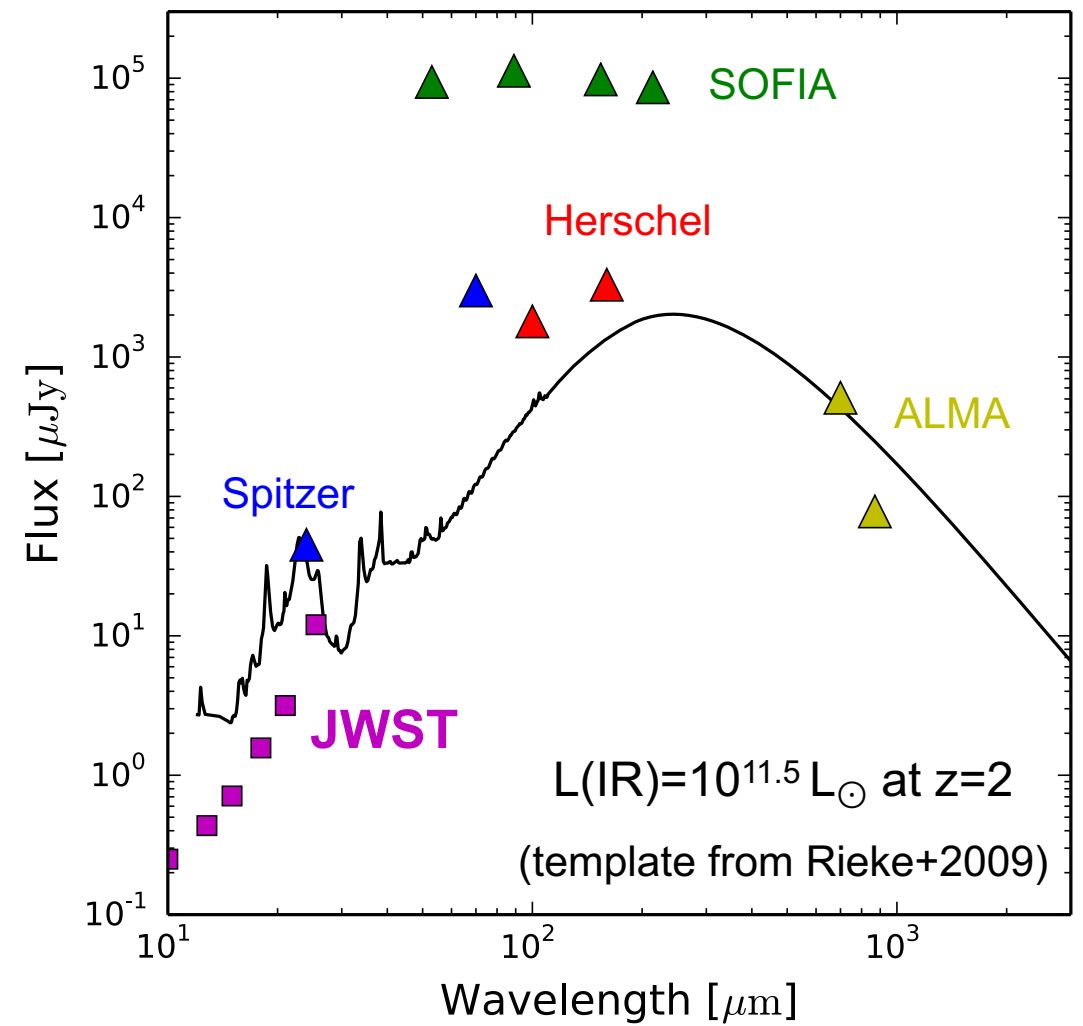
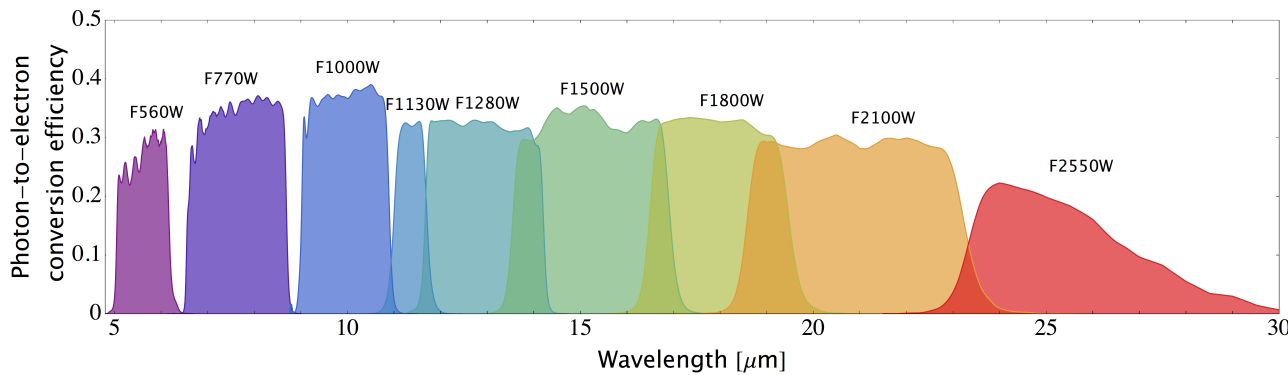
- **Imager**
- **LRS**: low-resolution spectroscopy ( $R \sim 100$ )
- **MRS**: medium-resolution integral field unit (IFU) spectroscopy ( $R \sim 1550 - 3250$ )
- **Coronagraphy**



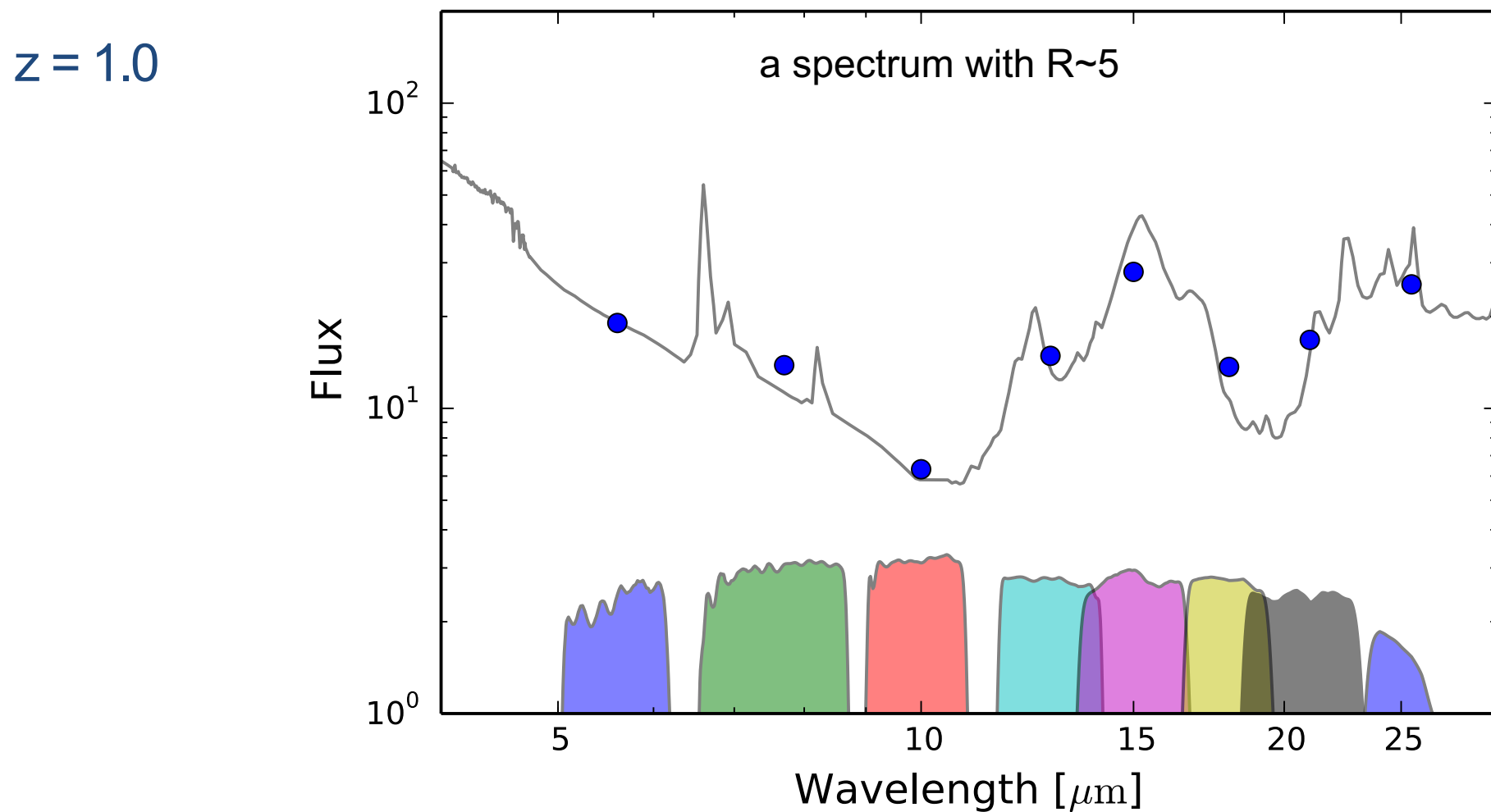
See: Wright et al. 2015, Rieke et al. 2015

## JWST MIRI Imager

- 9 filters at  $4.9 - 28.8 \mu\text{m}$
- Pixel scale:  $0.11 \text{ arcsec/pix}$ 
  - At  $25 \mu\text{m}$ : FWHM of  $0.82 \text{ arcsec}$
- Field of view:  $74 \times 113 \text{ arcsec}$



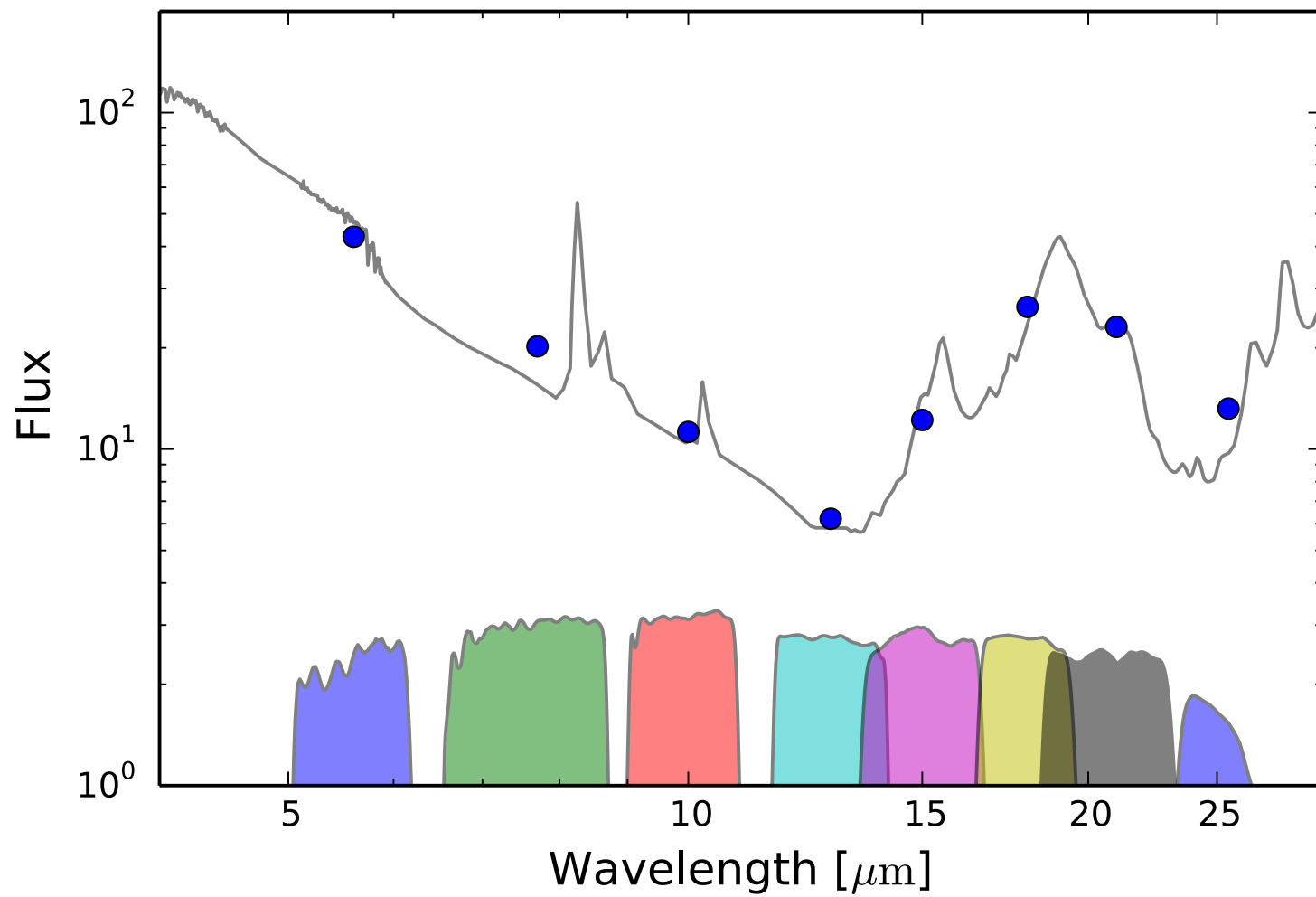
## Tracing multiple PAH components:



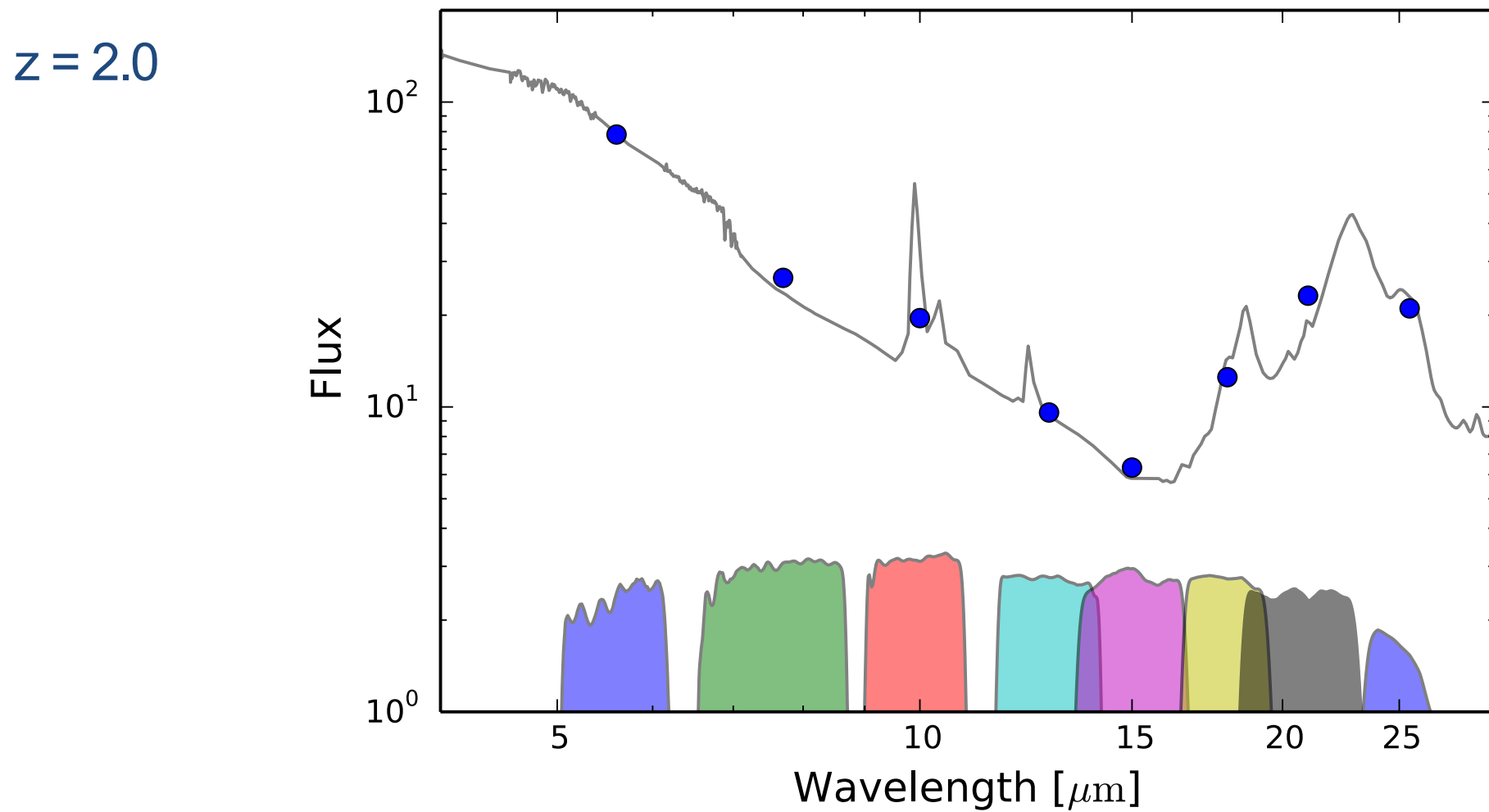
Also see: JWST/MIRI US extragalactic GTO program (PI: G. Rieke, Co-Is: S. Alberts, J. Lyu, J. Morrison, I. Shivaei)

## Tracing multiple PAH components:

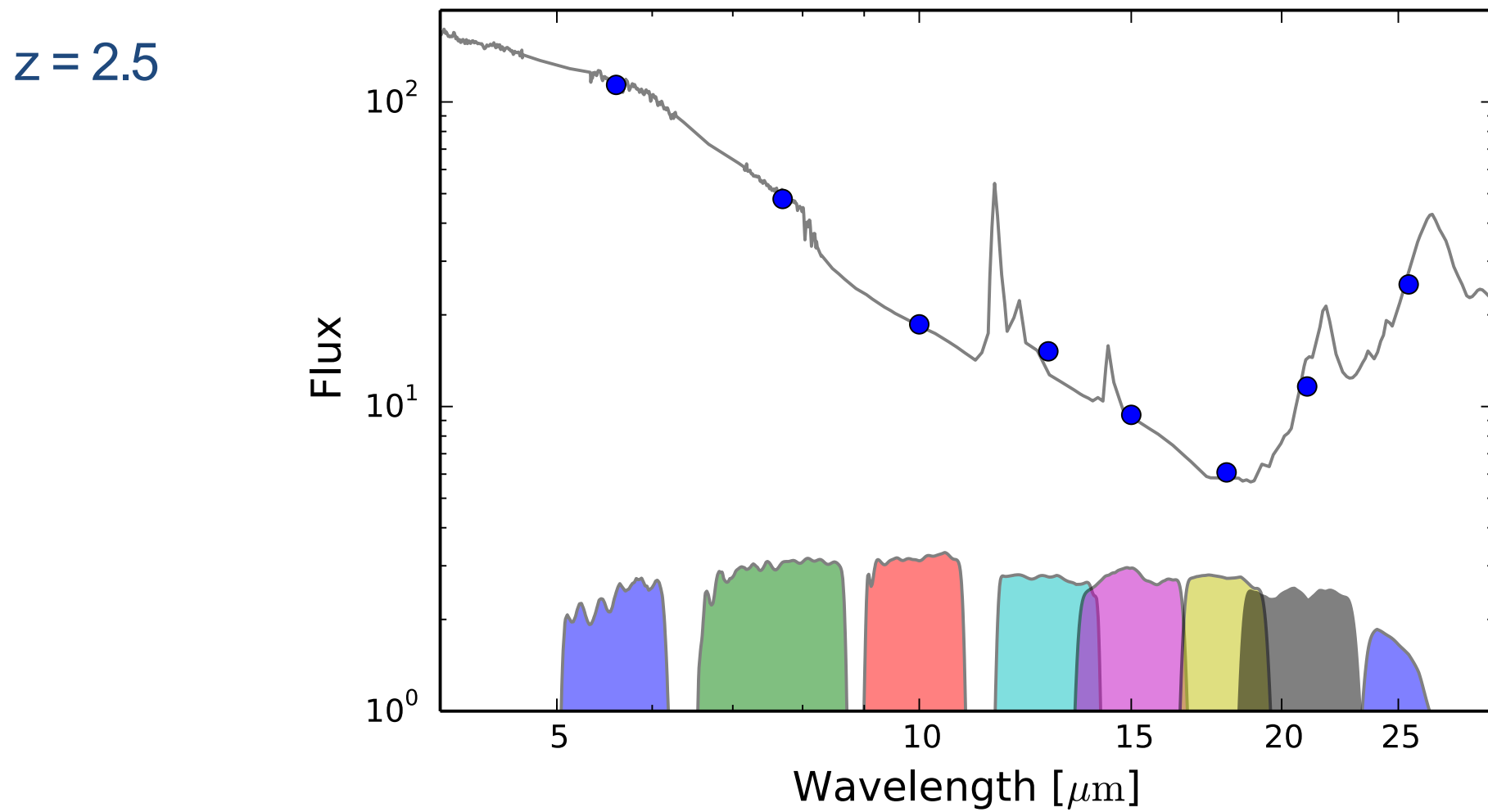
$z = 1.5$



## Tracing multiple PAH components:

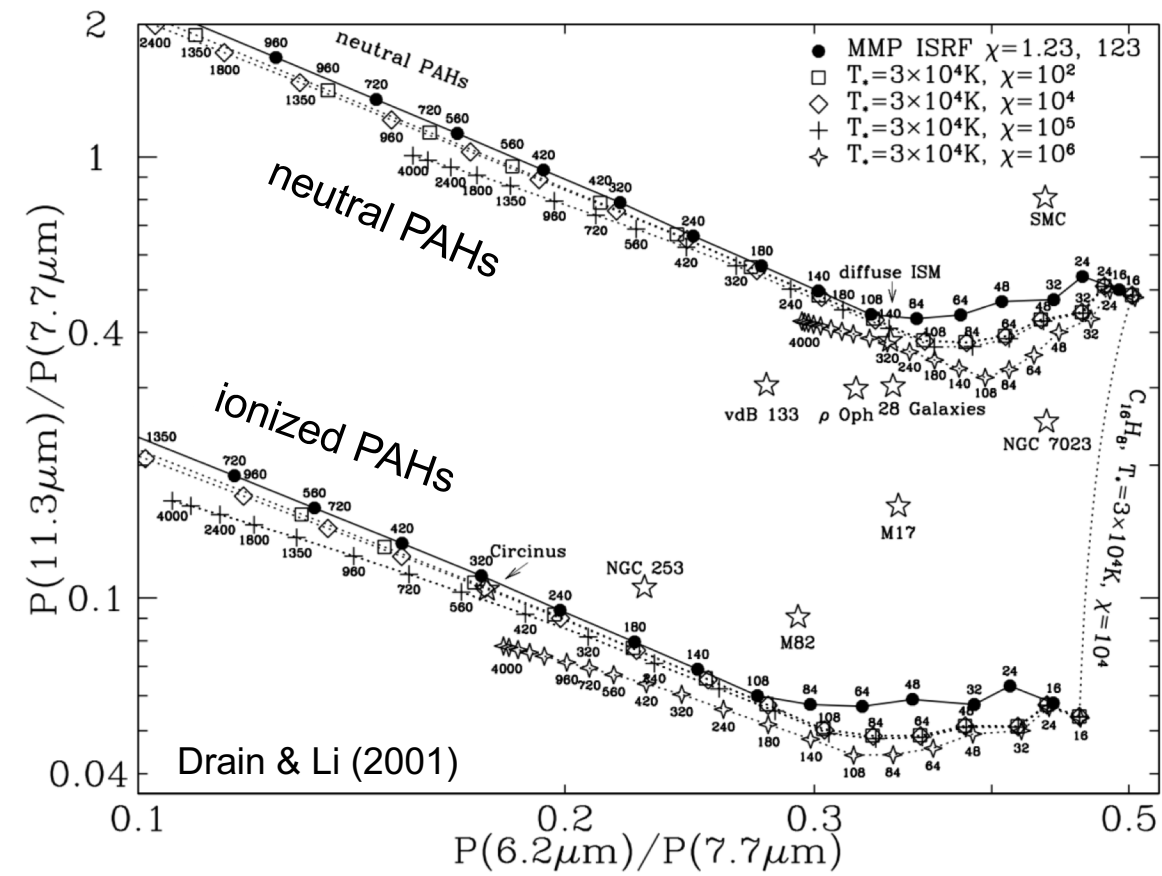
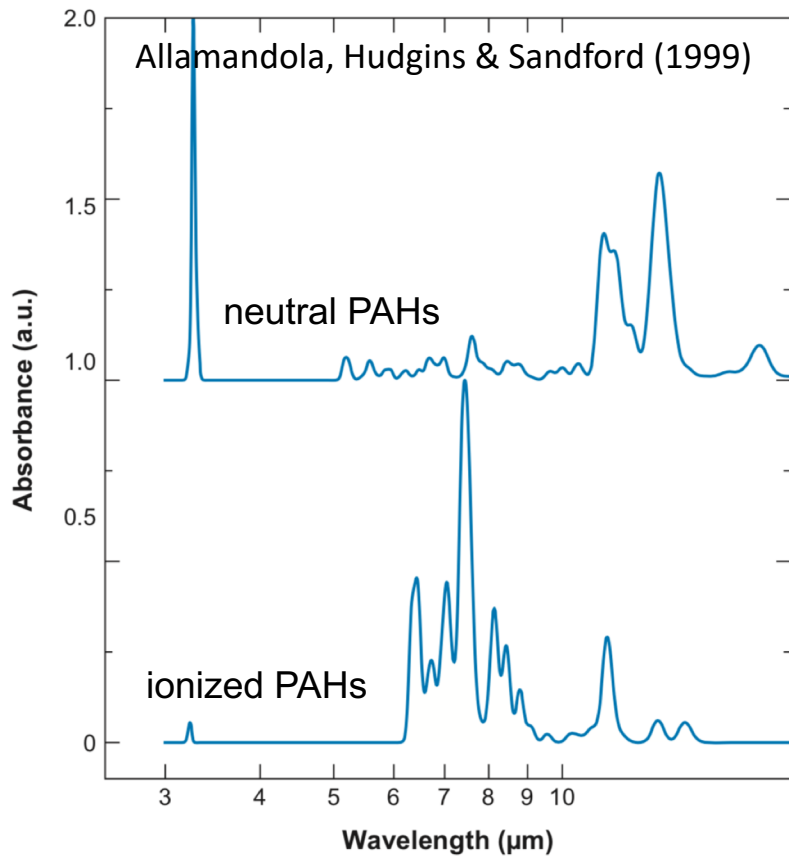


## Tracing multiple PAH components:



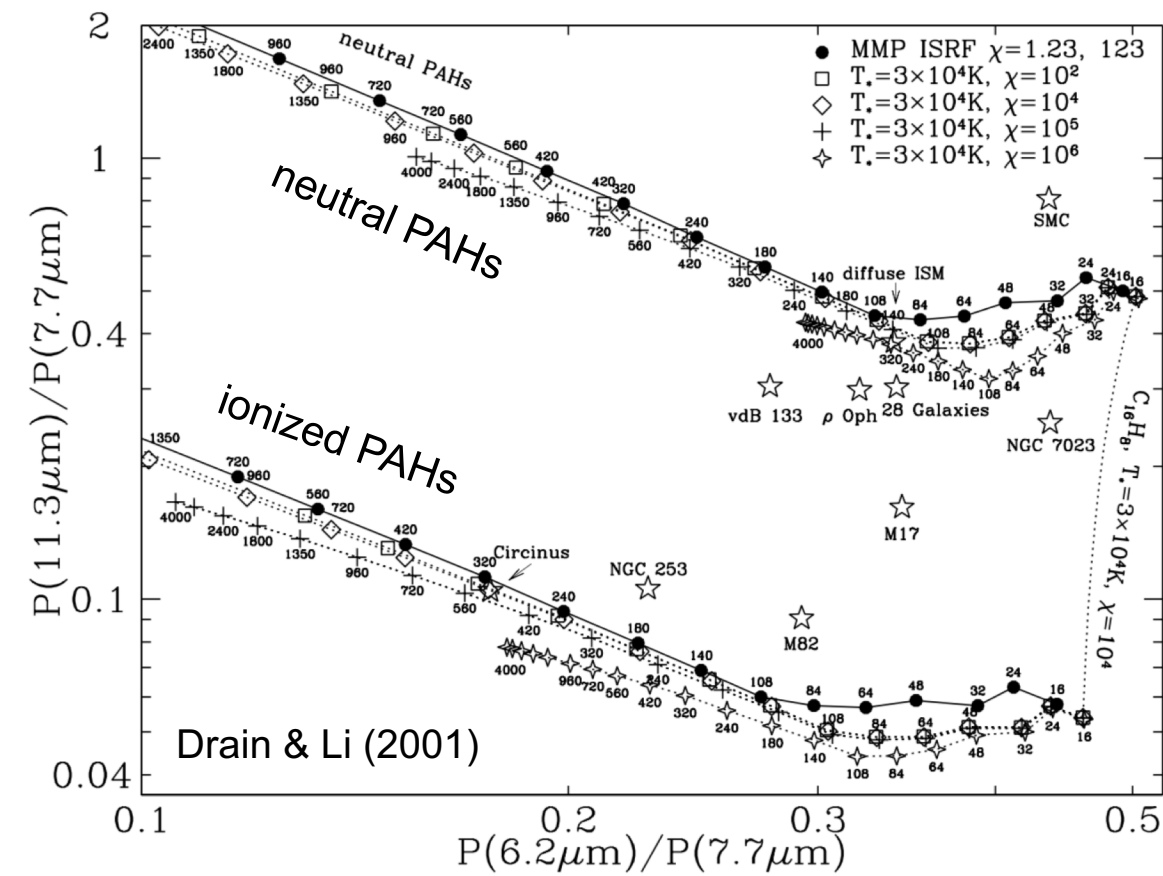
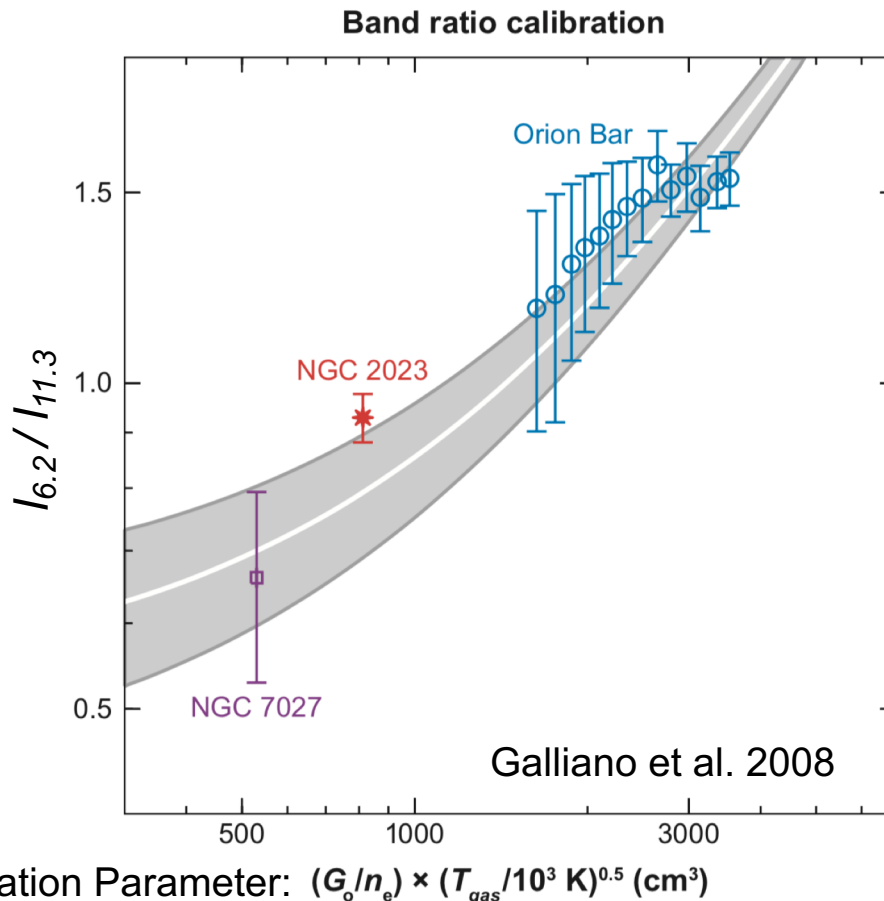
# What can we learn from the relative intensities of aromatic features?

- PAH charge, size, and molecular structure



What can we learn from the relative intensities of aromatic features?

- PAH charge, size, and molecular structure
  - Conditions of ISM and properties of the emitting sources

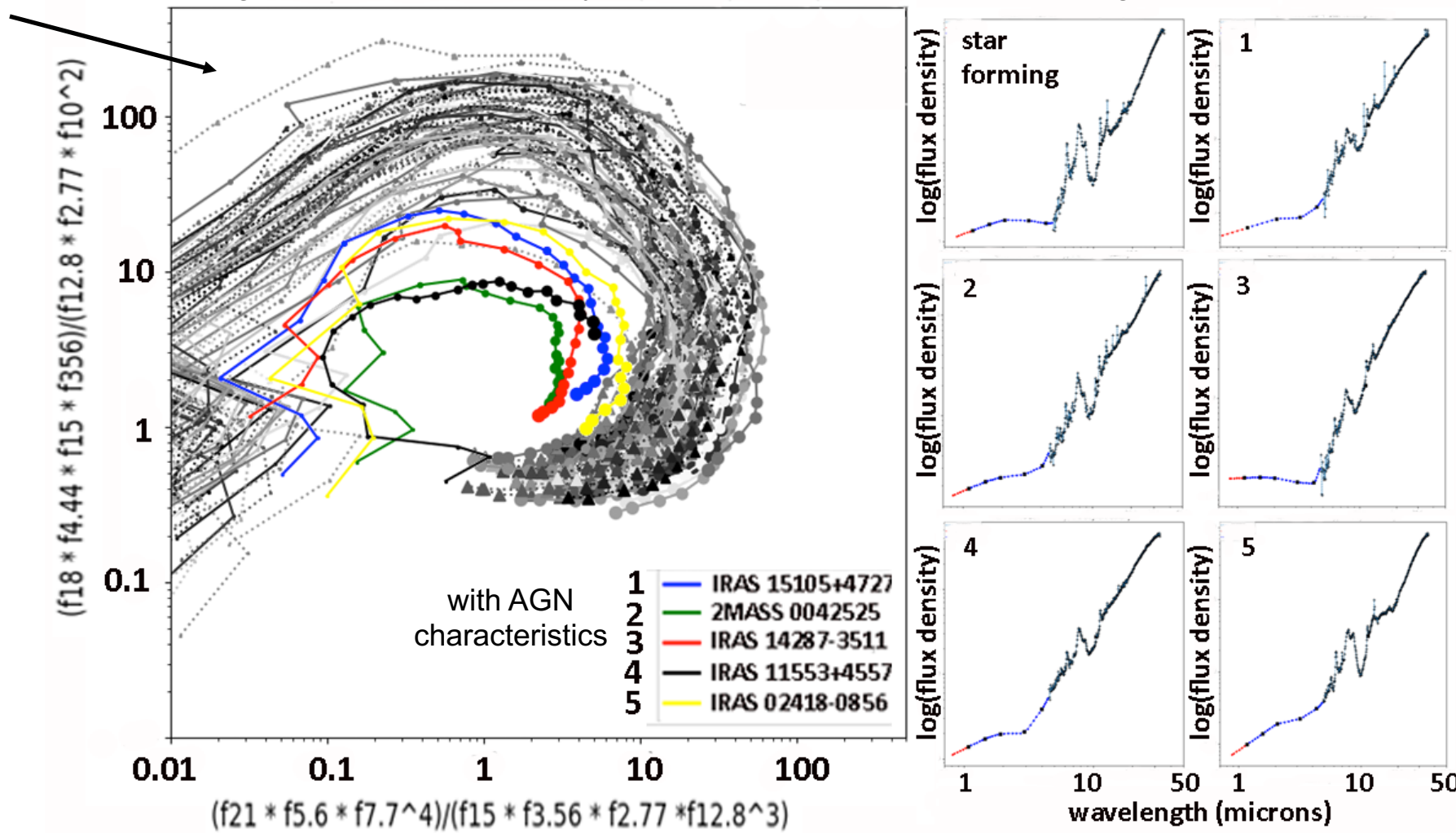


See also: Tielens 2008, Smith et al. 2007, Draine & Li 2007, Peeters et al. 2002, Hony et al. 2001

# MIRI and NIRCam multi-color diagrams to identify sources with embedded AGN

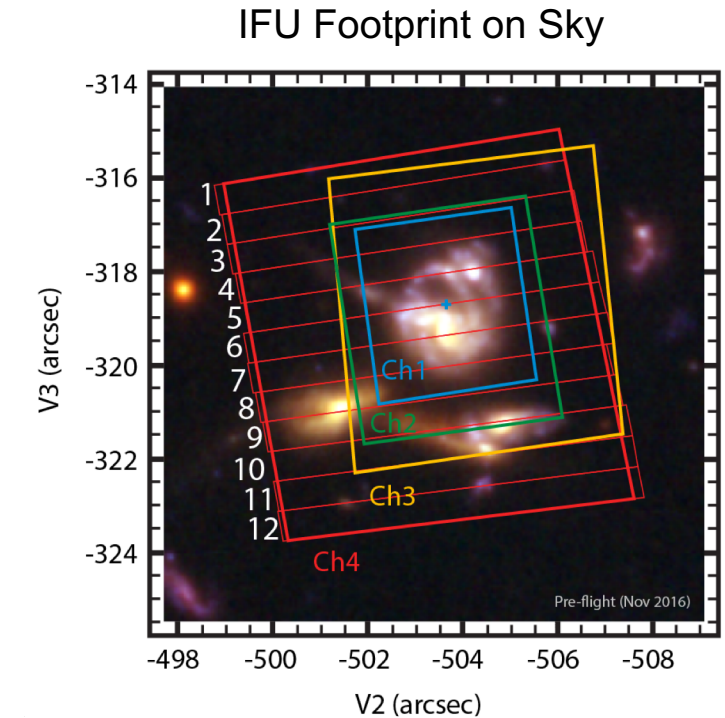
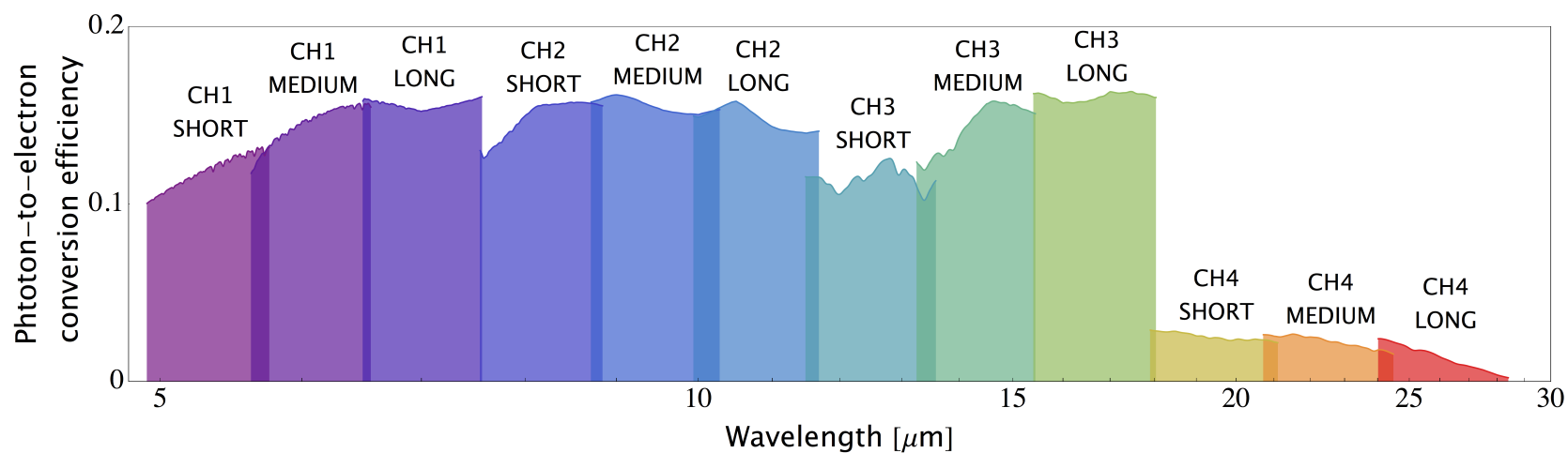
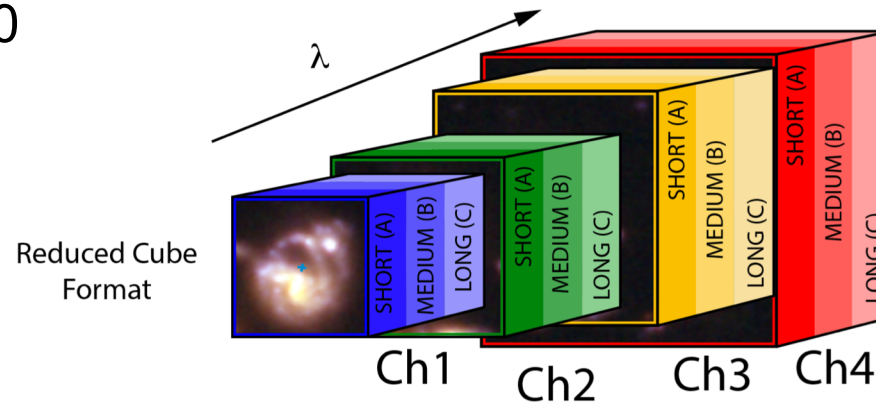
Star-forming  
galaxies at  
 $z = 0.5 - 2.4$

Image Credit: G. Rieke, J. Lyu, J. Morrison; JWST/MIRI GTO program

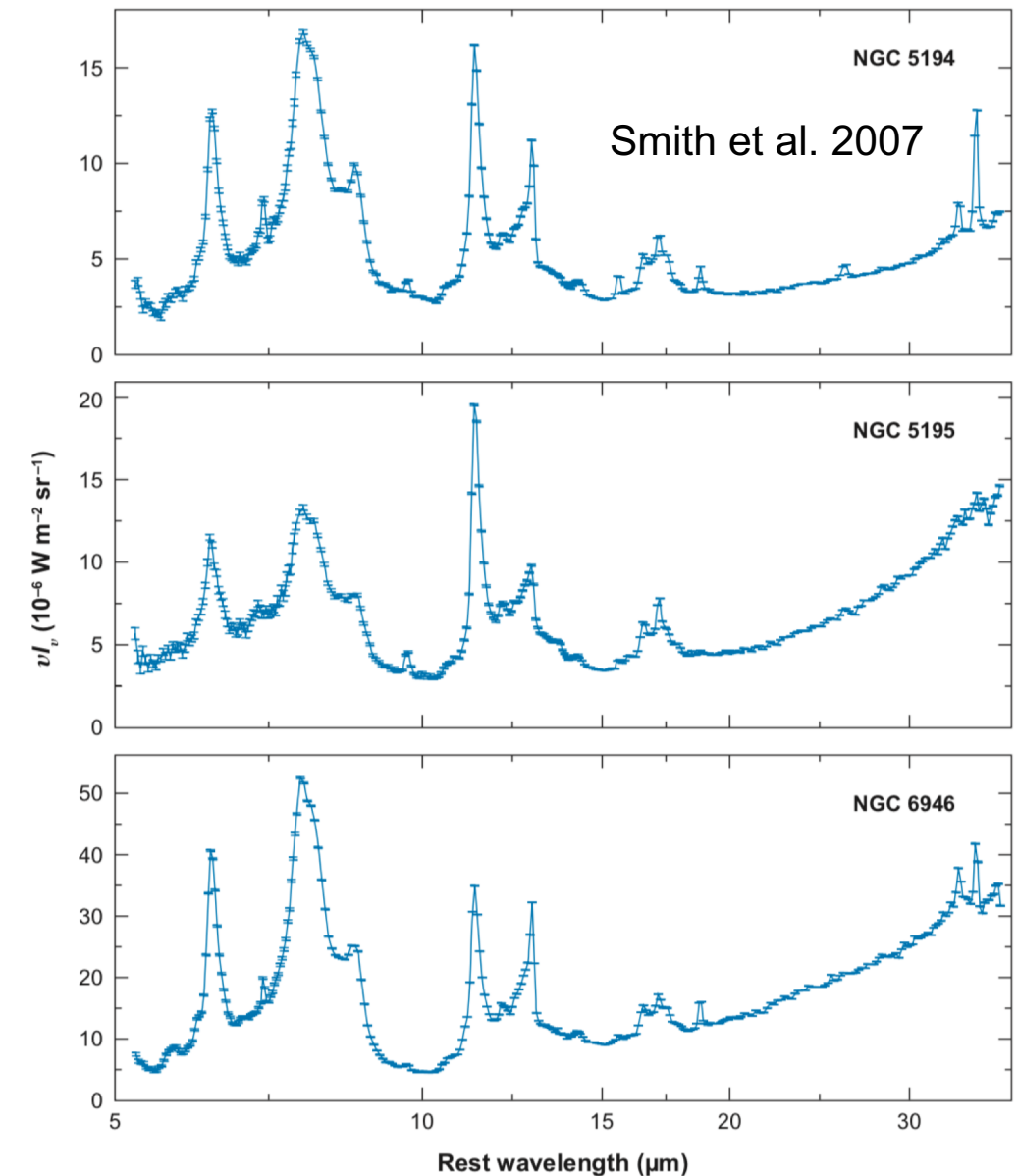
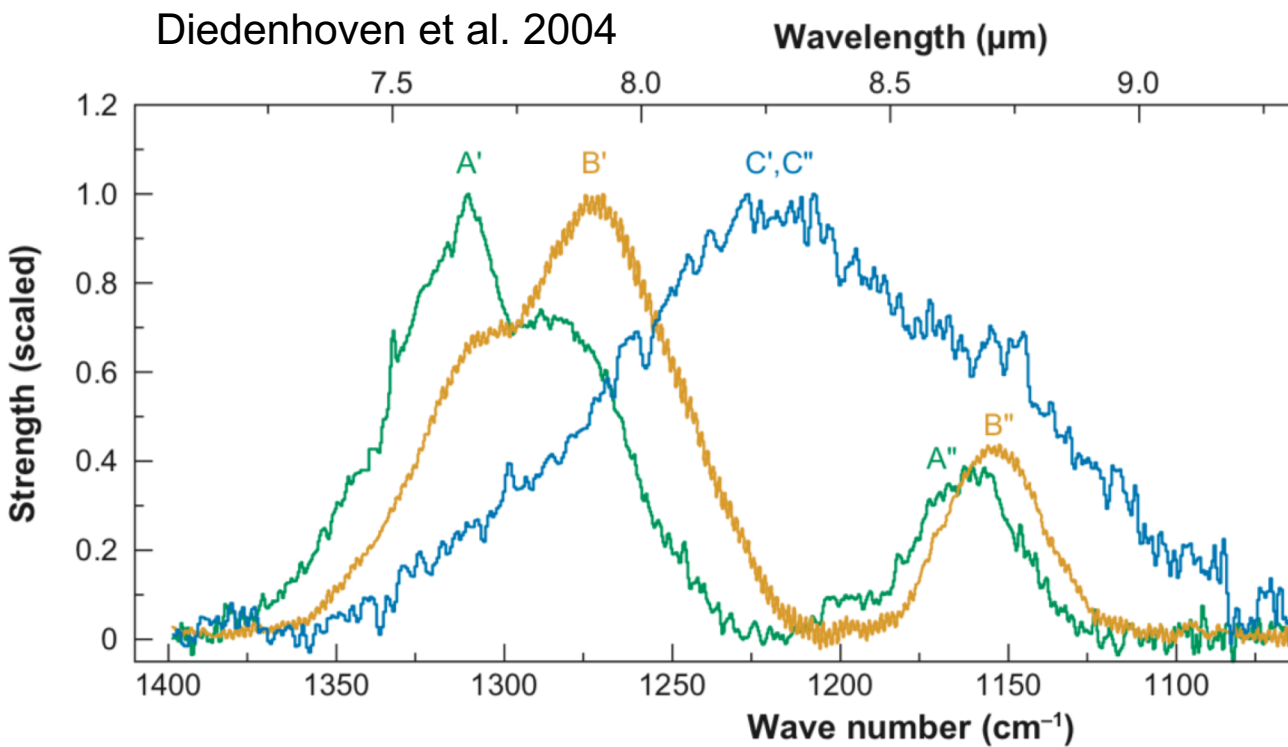


# JWST MRS: Medium Resolution Spectroscopy

- Four separate IFUs, called channels 1, 2, 3 and 4
- 5 to 28.5  $\mu\text{m}$
- $R \sim 1550\text{--}3250$

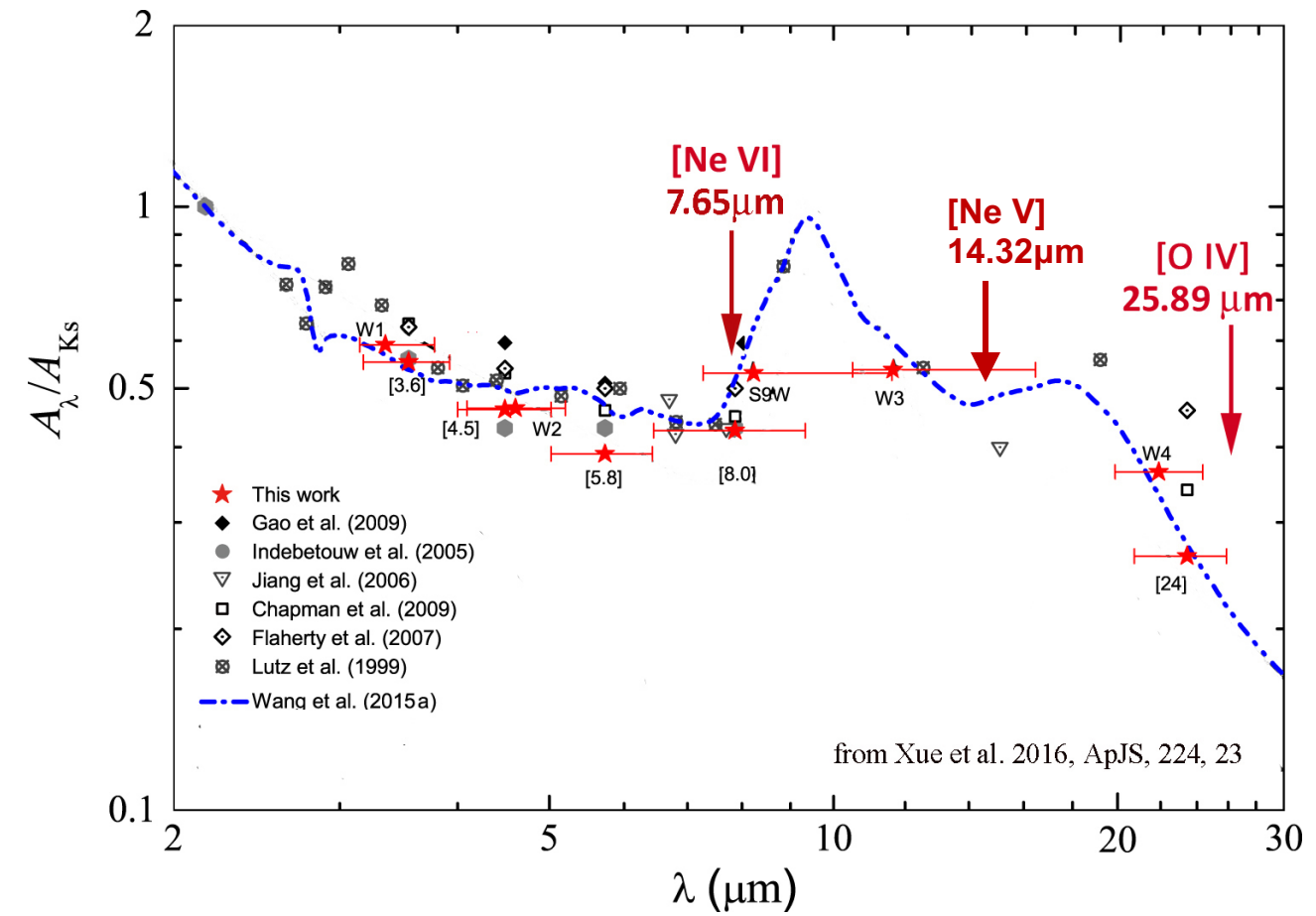
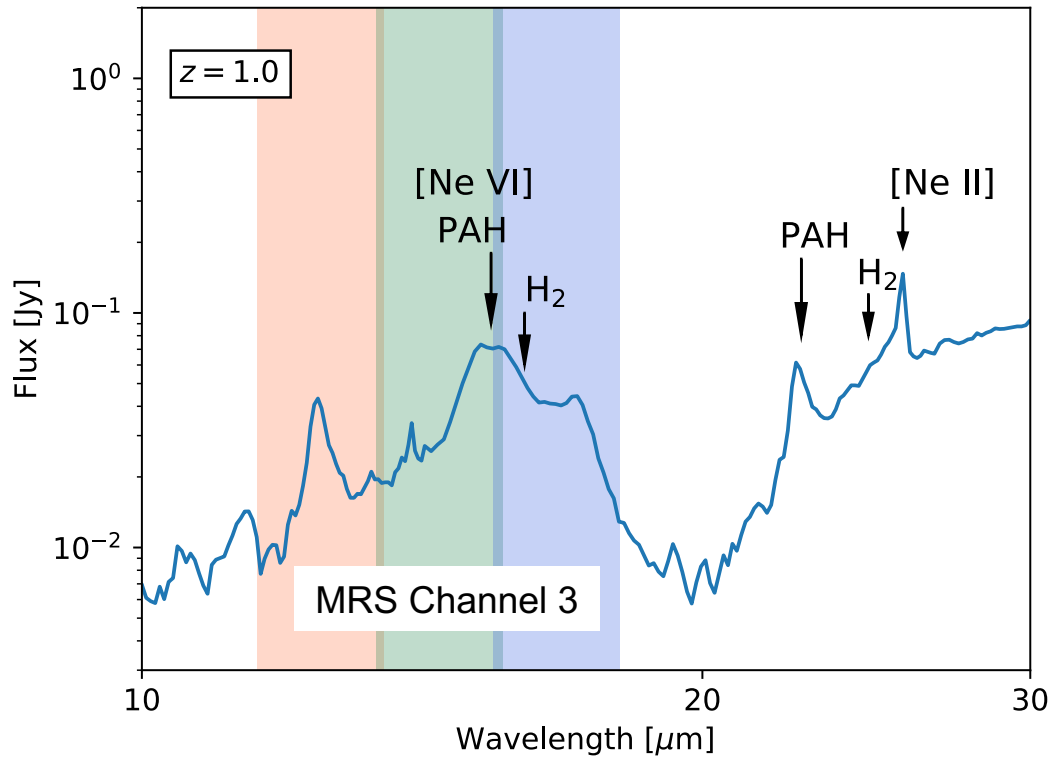


## Aromatic bands spectra: variations in the profile and peak position

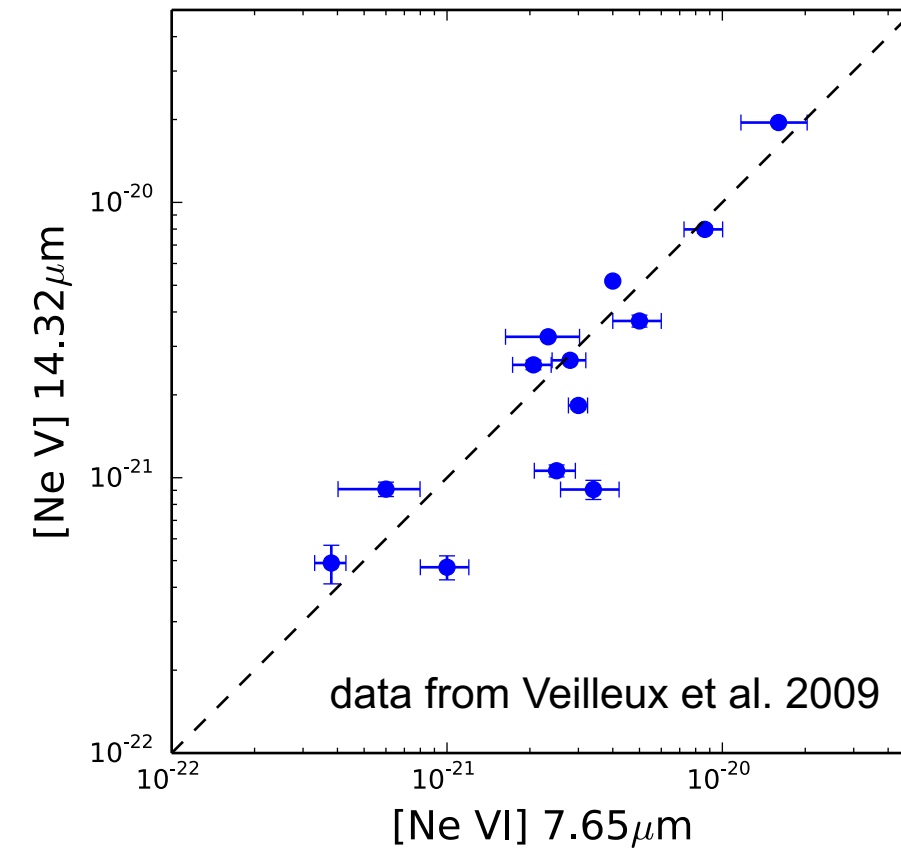
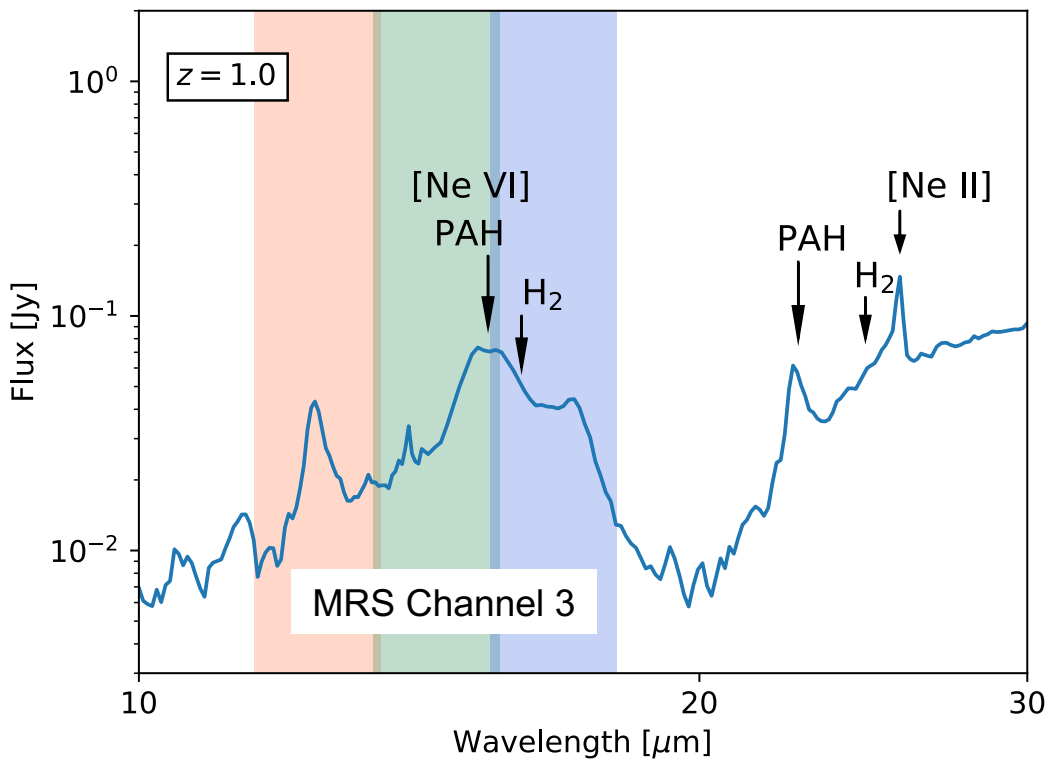


See also: Peeters et al. (2002); Sloan et al. (2007), Tielens (2008)

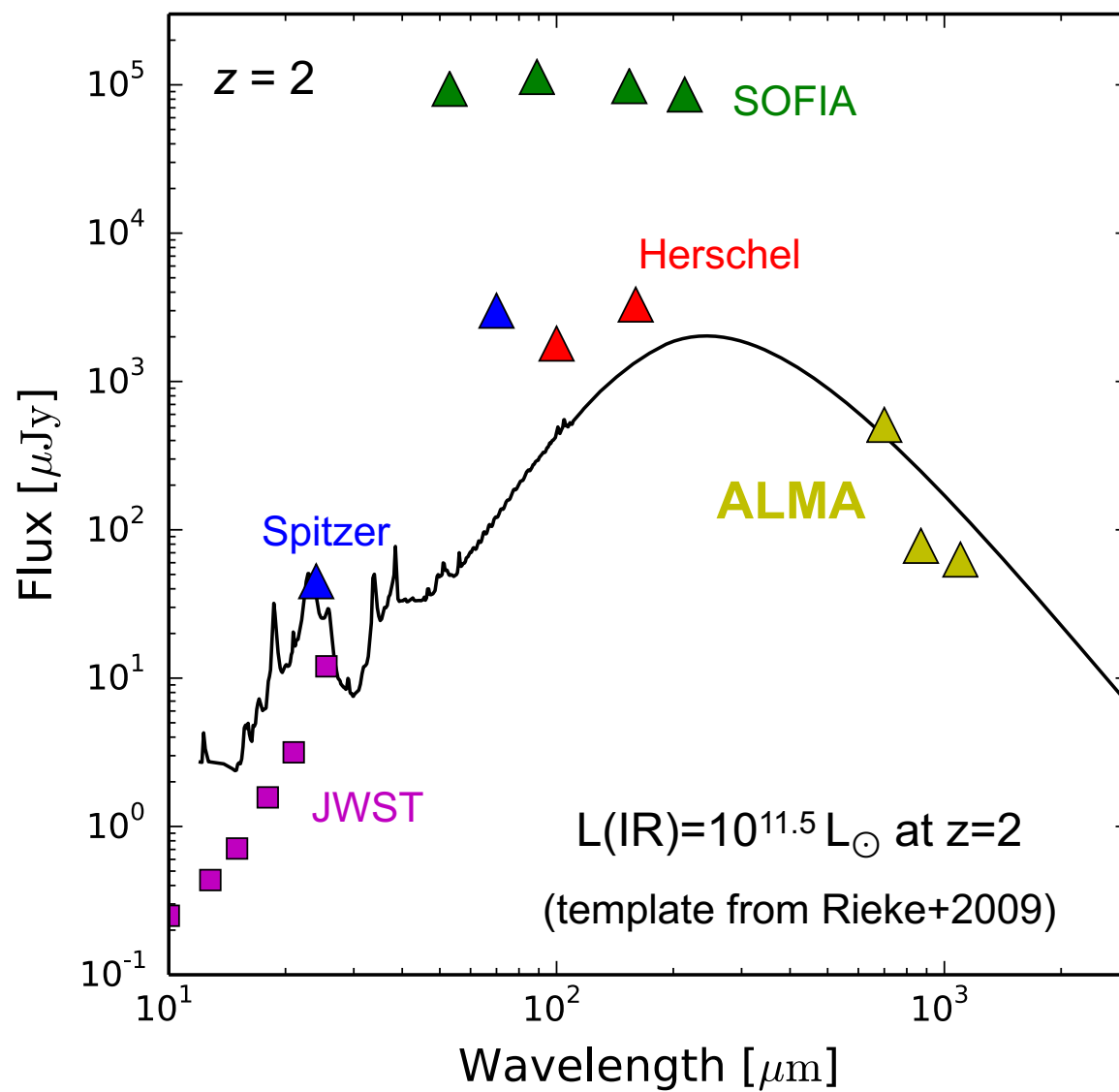
# Pulling the AGN needle out of the star formation haystack: Using [N VI] 7.65 $\mu$ m fine structure line (ionization potential of 158 eV)



# Pulling the AGN needle out of the star formation haystack: Using [N VI] 7.65 $\mu$ m fine structure line (ionization potential of 158 eV)

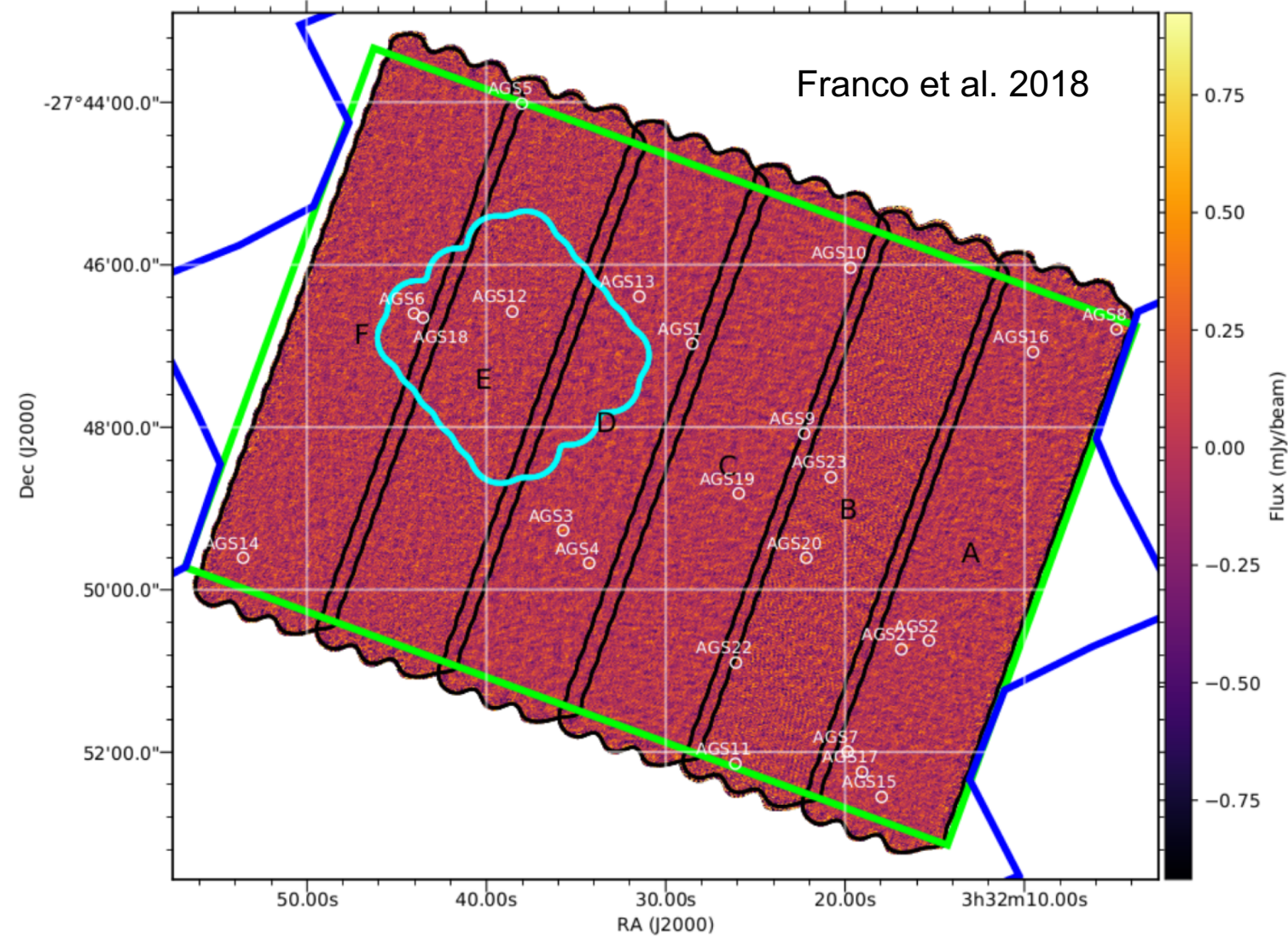


Moving to longer wavelengths to calculate total IR luminosity...



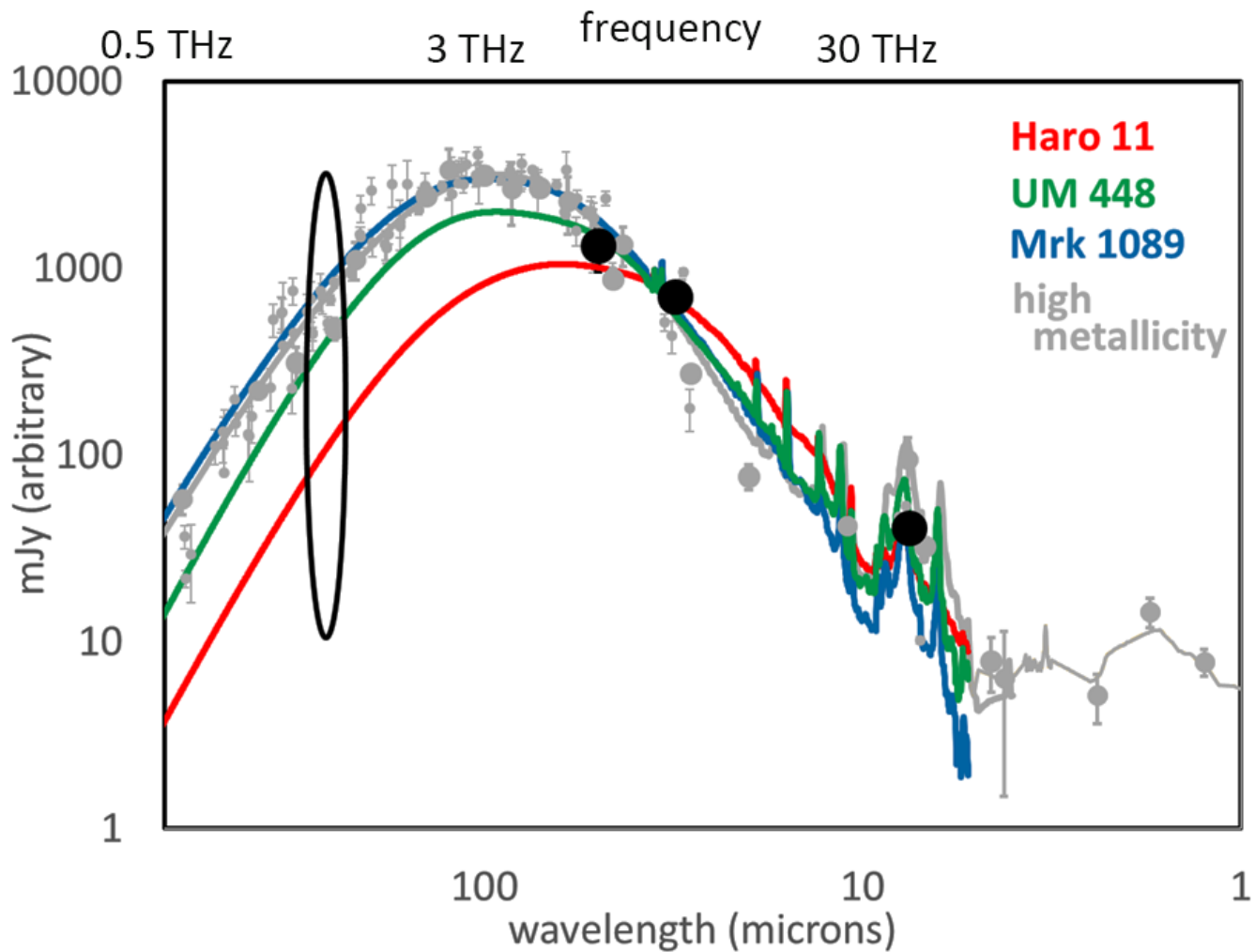
# GOODS-S ALMA 1.1 mm image

846-pointing mosaic  
~60 seconds per pointing



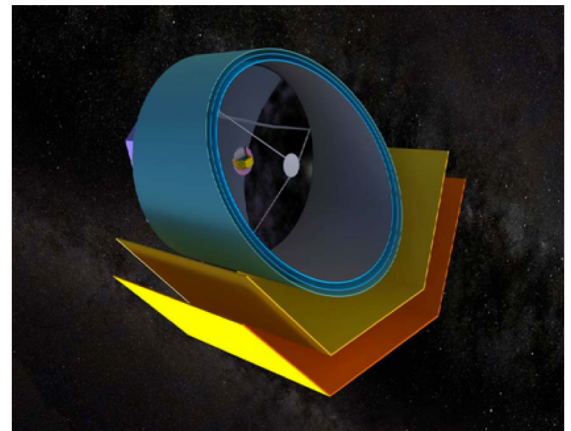
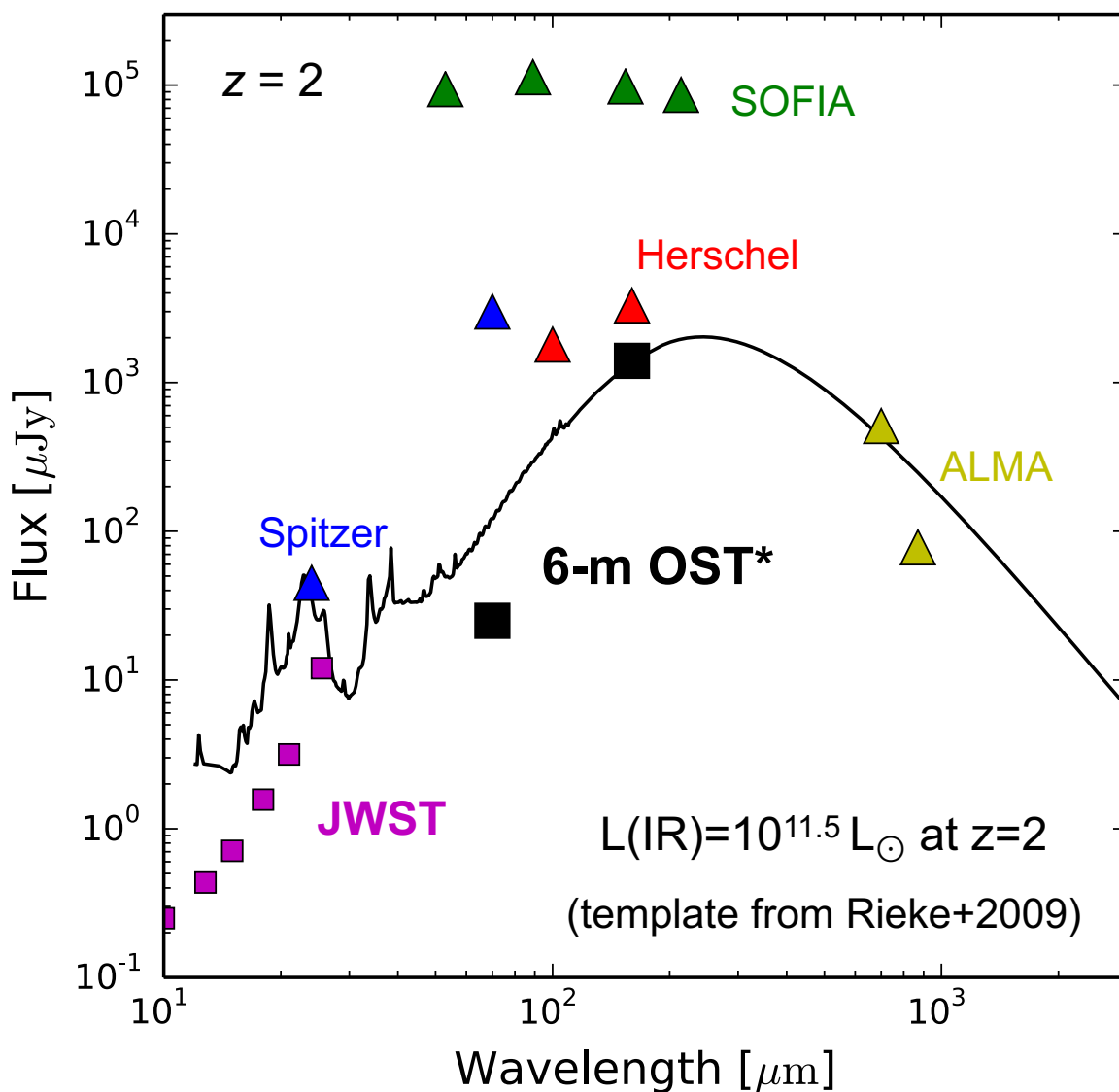
See also: Aravena et al. 2016, Scoville et al. 2016, Dunlop et al. 2017, Elbaz et al. 2018, Rujopakarn et al. 2016

## The large range of behavior in the far-IR emission of z~2 galaxies



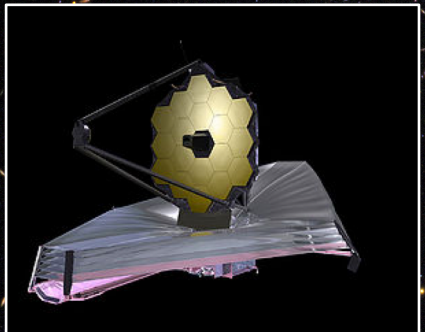
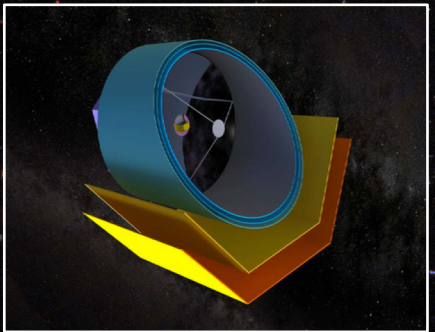
~ 0.8 dex variation in the observed 870  $\mu\text{m}$

## 6-m Origins Space Telescope Imager at 70 and 160 $\mu\text{m}$



\* Confusion-limited sensitivity calculations using SDC method; Dole+2003, 2004

# Summary



- ❖ For the foreseeable future, mid-IR aromatic bands will be the main indicators of the dust emission and obscured star forming regions at intermediate redshifts ( $z \sim 1-3$ )
  - PAH intensity is strongly dependent on metallicity, which suggests a higher sSFR at  $M_* < 10^{10} M_\odot$  and higher bolometric luminosity density and SFR density at  $z \sim 2$
- ❖ Future with **JWST/MIRI**:
  - MIRI imager: tracing PAH band ratios to characterize the PAH molecules characteristics and physical conditions of the emitting source, identifying embedded AGN
  - MIRI MRS: spectra of the aromatic bands, looking for [N VI] as a tracer of obscured AGN
- ❖ A 6-m **OST** can get accurate SFRs at  $z \sim 2$  (based on rest 24  $\mu\text{m}$ ) down to  $10^{11} L_\odot$ . Accompanied with **JWST**, it will be a powerful way to measure the aromatic bands on the same galaxies.

